Tetrahedron Vol. 48, No. 30, pp. 6175-6217, 1992
Printed in Great Britain

0040-4020/92 $5.00+.00
Pergamon Press Ltd

TETRAHEDRON REPORT NUMBER 318

Macrocyclic Polyamines with Intelligent Functions.

Eiichi Kimura

Contribution from the Department of Medicinal Chemistry, School of Medicine, Hiroshima University, Kasumi, Minami-ku 1-2-3, Hiroshima 734, Japan

(*Received* 24 *April* 1992)

Contents

1. Introduction

Saturated macrocyclic polyamines have been long known. In fact, the history goes back to 1960 s',[1-3] while macrocyclic polyethers ("crown ether")[4] have not been discovered yet. Until early 1970 s', macrocyclic polyamines had been used mostly as chelating agents for transition metal ions for study of basic coordination chemistry.[5,6]

As the study has developed, these macrocyclic polyamines (*e.g.* cyclam **1**) were discovered to possess some common properties as those of nitrogen-containing biofunctional molecules (Figure 1) such as porphyrins,[5] peptides (*e.g.* Gly-Gly-His),[7,8] or biogenic polyamines (*e.g.* spermine)[9,10] and even more variety of functions.

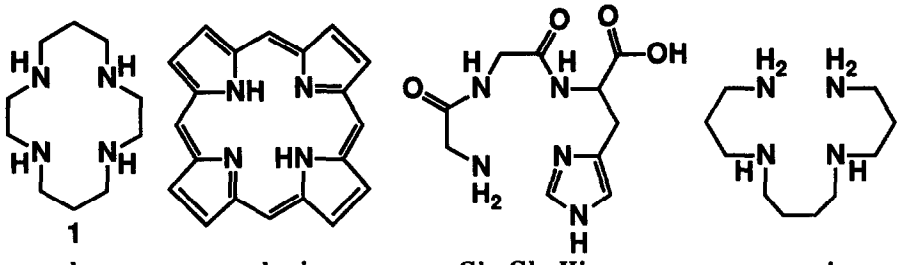

Figure 1.

The major difference in functions of macrocyclic polyamines from those of crown ethers derives from the composite nitrogen donors and their strong basicities. Accordingly, macrocyclic polyamines are highly protonated and strongly bind with transition metal ions and heavy metal ions *via* coordination. Moreover, upon cyclization, polyamines gain new properties beyond those anticipated from mere assemblies of amines or linear polyamines.

This is best illustrated by the behaviors towards acids, *i.e.* protons and metal ions. With macrocyclic polyamines, due to the restricted conformation, the nitrogen lone pairs may overlap to bring about higher electron densities in the macrocyclic cavities. Thus, the proton affinities at the initial stage are unusually high, *i.e.* p*K*a values are higher than ~10 known to ordinary, isolated secondary amines. In fact, some polyamines (*e.g.* [12]aneN3 **2**[11]) and its derivative **3**[12] are as basic (p*K*a > 13) as "proton sponge" (*e.g.* **4**).

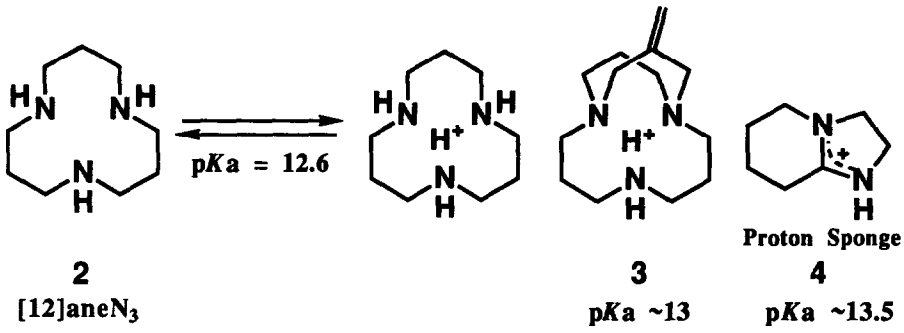

On the other hand, once protons are incorporated into the macrocyclic cavities, no more electron clouds are spared from (yet) unprotonated amines, and/or the already protonated amines are so close (due to the macrocyclic conformational restraint) that the proton affinities at the later stages are extremely weak. Compare the following protonation constants log K values for a linear, 2, 3, 2-tet **5** and macrocyclic cyclam **1** (Figure 2).[13]

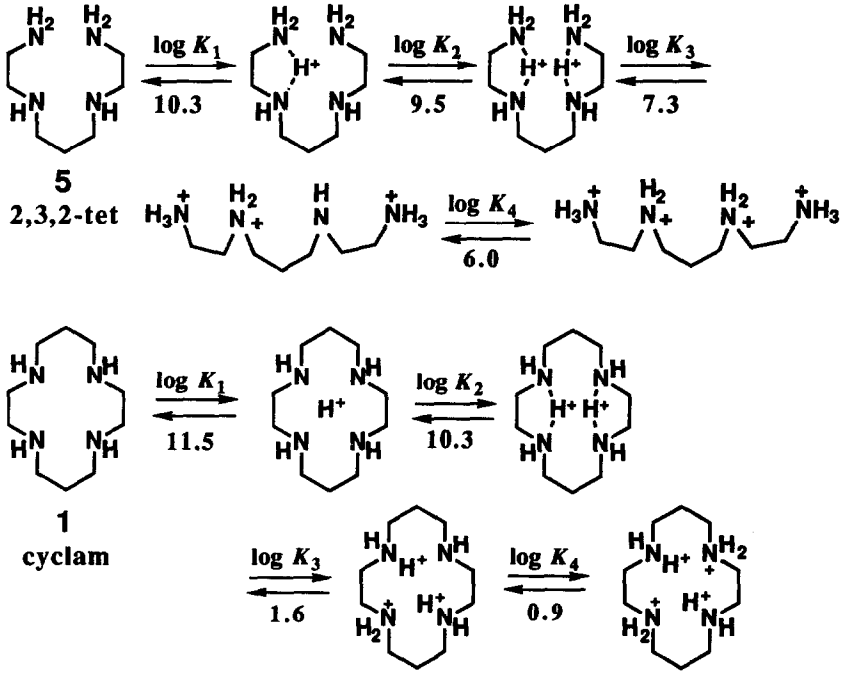

Figure 2. Comparison of protonation constants Ki for 2,3,2-tet 5 and cyclam 1

Macrocyclic structure is also extremely favorable for metal complexation. In terms of entropy factor, this may be viewed as an extension of the "chelate effect" (*i.e.* favorable entropy terms ΔS) that is a major contribution to an increase in complex stability as the number of chelate rings increases. See the following example (Figure 3).

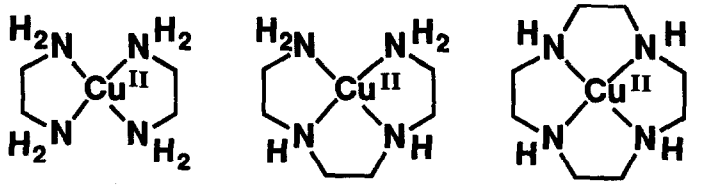

	$\log K_{CuL}$ = 20.2	$\log K_{CuL}$ = 24.8
ΔH = -25.5	ΔH = -21.6	ΔH = -18.3
ΔS = 7	ΔS = 19.5	ΔS = 51

Figure 3. Comparison of ΔH and ΔS in formation of Cu^{II}-N_4 complexes[14]

However, the best fitness of size for metal ions and macrocyclic cavity without any other configurational constraint gives the complexes with highest stability. This is the case for cyclam, [14]aneN$_4$ **1** ; compare the following complexation constants for [13]aneN$_4$ **6** and [15]aneN$_4$ **7** (Figure 4).

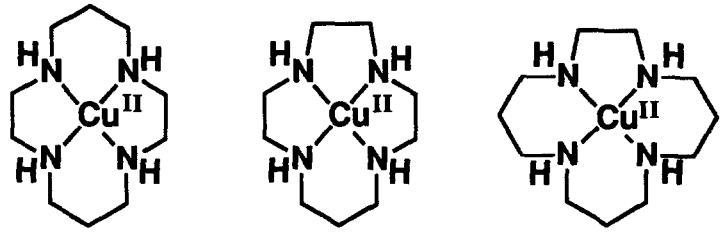

1	6	7
$\log K$ = 30.5[15]	$\log K$ = 29.1[16]	$\log K$ = 24.4[17]
	ΔH = -29.2	ΔH = -26.5
	ΔS = 34	ΔS = 23

Figure 4. Comparison of Cu^{II} complexation parameters for 13-15 membered tetraamines

It is extremely interesting that although (nonsubstituted) cyclam in general yields the most stable complexes with metal ions, the most stable tetra-substituted (containing donor atoms; *e.g.* -CH_2CO_2H) tetraaza macrocyclic complexes are generated always from cyclen **8** (Figure 5).[18] This is due to the limited freedom to fix the substituted donors to the most favorable coordination sites.

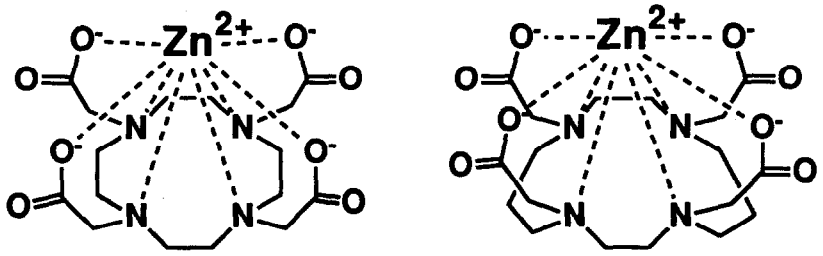

8 **9**

$\log K_{ZnL} = 21.1$[18] $\log K_{ZnL} = 16.3$[19]

Figure 5. Comparison of Zn^{II} complex stability for cyclen- 8 and cyclam-tetraacetates 9

One can design highly functional molecules by taking full advantages of those basic characteristics of macrocyclic polyamines. For instance, very distorted metal complexes could be constructed due to the extraordinary macrocyclic stabilities. Reaction intermediates, reaction transition states or extremely reactive molecules may also be designed. In other words, new metal catalysts or metalloenzyme models may be easily tailored from the basic macrocyclic structures.

The secondary amine donors in macrocyclic polyamines can synthetically be substituted with amides or with other heteroatoms, which may also act characteristic donors. These simple structural modifications would dramatically alter the complexing behaviors.

While macrocyclic polyamines thus act as host molecules for protons and metal cations, upon protonation (at neutral pH) polyamines now come to form complexes with anions[10] (Figure 6).

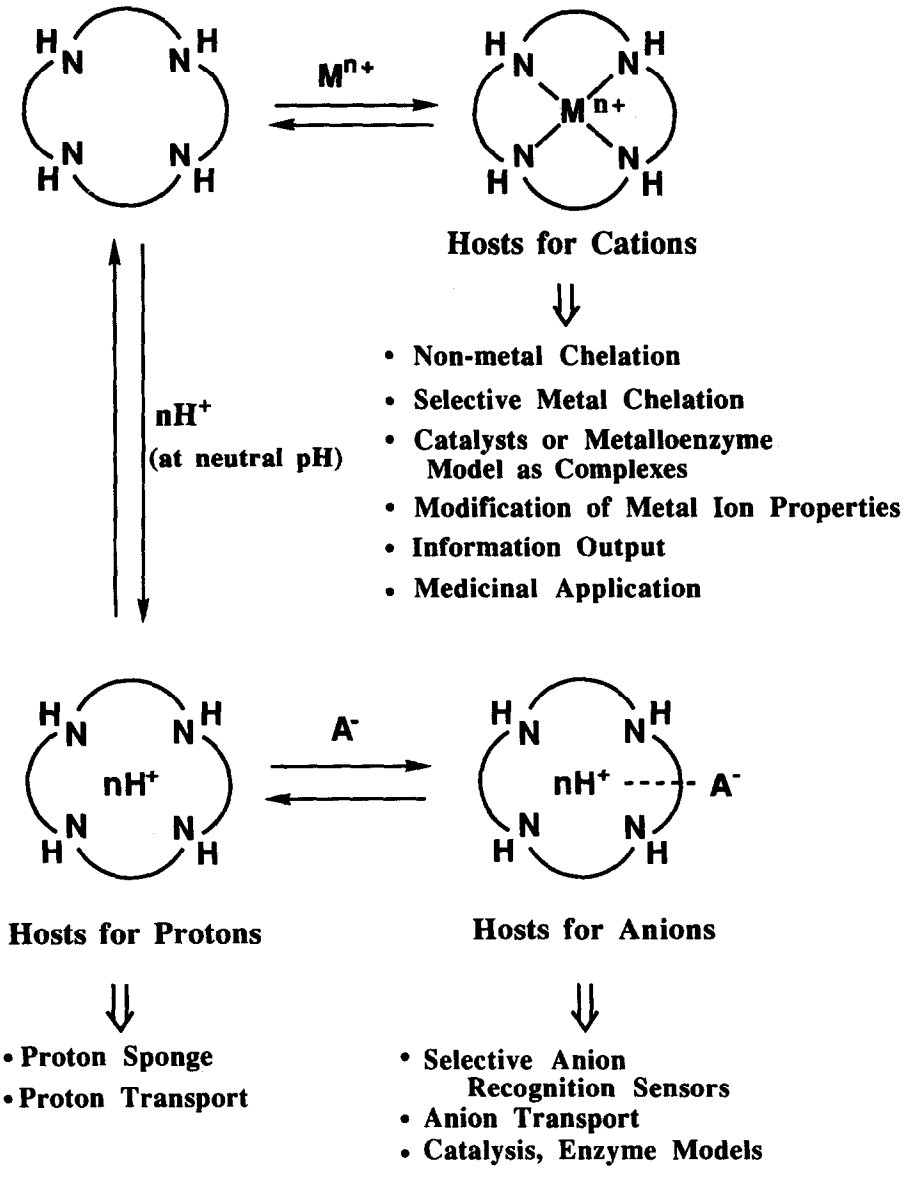

Figure 6. Characteristic properties of macrocyclic polyamines and their applications

The polyamine host-guest interaction would develop into more highly advanced chemical functions for (1) Design of more sophisticated hosts for more selective and efficient uptake of

wider ranges of guest molecules and ions; (2) Selective separation, dissolution and membrane transport of guests; (3) Information input or output upon host-guest interaction; (4) New functions as complex assemblies; (5) New chemical reactants or catalysis due to host-guest interactions and (6) Recognition of external stimulus and/or messages to initiate above functions (*i.e.* attachment of robotic functions). The following chapters will illustrate these new explorations of chemistry recently developed in our laboratory.

2. Selective Uptake and Transport of Metal Ions

2.1. *New Hybrid Molecules of Cyclam and Oligopeptides*

Macrocyclic polyamines (L) can complex with virtually all kinds of heavy metal ions and transition metal ions. However, these complexes ML^{n+} are generally so stable ($\log K_{ML} > \sim 15$) that they cannot practically be used as *selective* metal chelating agents. For instance, one could not anticipate outstanding correlation between ring cavity size and metal ion size as often found for crown ethers with alkaline metal ions (in nonaqueous solvents).[4] Another disadvantage with the strong complexation is the lack of reversibility; *i.e.* the metal dissociation is so slow that recovery of metal ions from complexes is nearly impossible. As a consequence, macrocyclic polyamines cannot be used as membrane carriers for metal ions.

We thus have designed *dioxocyclam* **10** that contains two amide functions in cyclam (Figure 7).[7] The original idea came from the Cu^{II}-carrier proteins that were known to carry Asp-Ala-His at the N-terminal amino acid composites (Figure 8).[7,19,20]

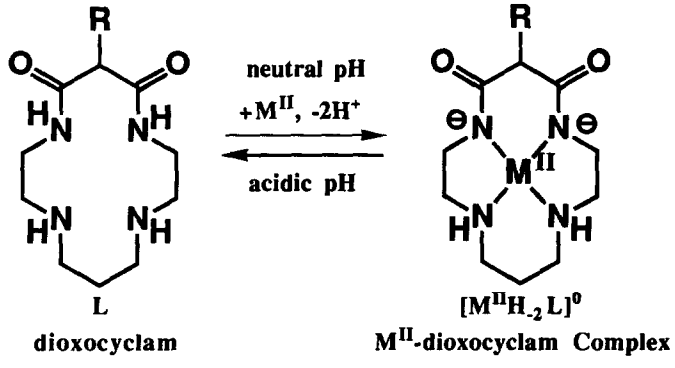

Figure 7. Reversible M^{II} uptake by dioxocyclam 10

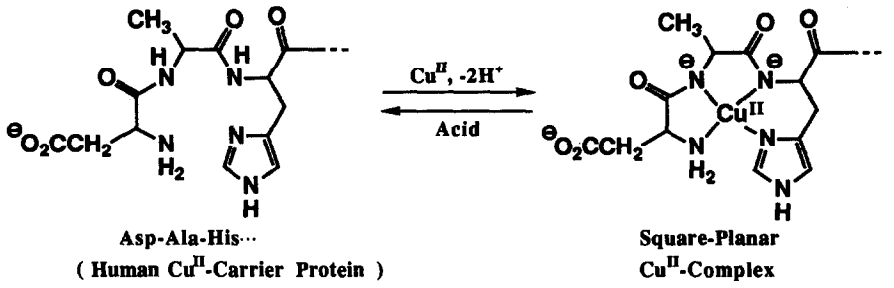

Figure 8. Reversible Cu^{II} uptake by an N-terminal tripeptide (Asp-Ala-His) of proteins[19]

Dioxocyclam **10** was found to entrap only Cu^{II},[7] Ni^{II},[21] Co^{II},[22] Pd^{II},[23] and Pt^{II} [23] among (+2) transition metal ions tending to take an N_4 square-planar configuration, with concomitant dissociation of the two amide protons at neutral pH (Figure 7). These complexes $[MH_{-2}L]^0$ **11** were isolated as stable crystalline products. Upon addition of acid (*e.g.* 0.1 M

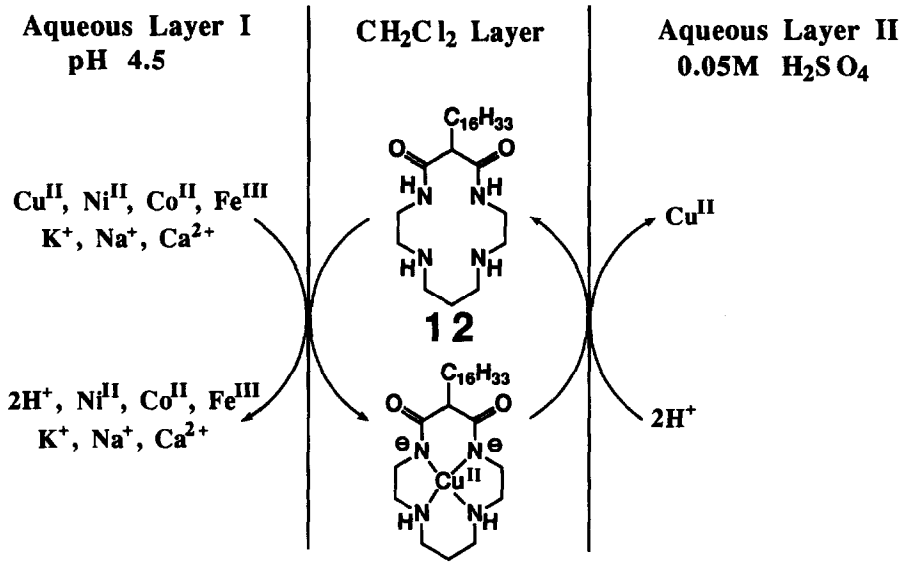

Figure 9. A new device for liquid membrane transport of Cu^{II}, accompanied by H^+-countertransport

HCl aqueous solution), the complex decomposition occurs with complete recovery of the dioxocyclam **10** and M^{II} (Figure 7). The measured stability constants for dioxocyclam (log $K(MH_{-2}L) = [MH_{-2}L][H^+]^2 / [M^{II}][L]$) are 1.0 (M = Cu),[7] -5.5 (Ni),[2] and -11.4 (Co)[7,21] which disclose appreciable difference among the metal ions. Together with the outstandingly fast kinetic advantage, one could devise a Cu^{II}-selective membrane transport using a lipophilic dioxocyclam **12**[24] as depicted in Figure 9. From aqueous layer I to aqueous layer II, Cu^{II}-selective extraction is possible. A special feature of this transport is that unlike neutral crown ether carriers (where normally lipophilic anions such as picrate liquid membrane are used), no counteranions are needed. Moreover, the countertransport of protons accompanies in our device, which energetically drives the Cu^{II}-transport smoothly against the Cu^{II}-concentration uphill.

2.2. *New Dioxocyclams with $(N^-)_2S_2$ and $(N^-)_2S_3$ Donors. Novel Ligands Selective for Noble Metal Ions*[25,26]

We have recently extended the dioxocyclam to a new version that is composed of thiaethers in place of the amines.[25,26] These new diamide macrocycles **13** and **14** accommodate only noble metal ions Pt^{II} and Pd^{II}, but not common transition metal ions Cu^{II}, Ni^{II} or Co^{II} (which are all accommodated into dioxocyclam) in MeOH-H_2O (at pH < 10). Such selective recognition of noble metal ions against other common metal ions has no precedence. In these new macrocyclic ligands, the discriminating functions are endowed by the combination of the unique S donors and amide groups in the macrocyclic skeleton to concertedly work only on Pt^{II} and Pd^{II} ions.

Divalent noble metal ions Pd^{II} and Pt^{II} are known to possess somewhat mixed properties of hard and soft acids. Toward peptide ligands (to form square-planar complexes like M^{II}-dioxocyclam) their hard acidities are greater than those of Cu^{II} and Ni^{II}, so that Pd^{II} and Pt^{II} can displace the amide protons at lower pH than Cu^{II} or Ni^{II} can.[26] Toward soft ligands (*e.g.* sulfur donors) these noble metal ions can become soft acids and better fit than Cu^{II} or Ni^{II}.[30]

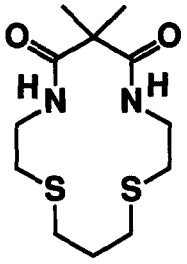

($\nu_{C=O}$ 1660 cm^{-1})

13

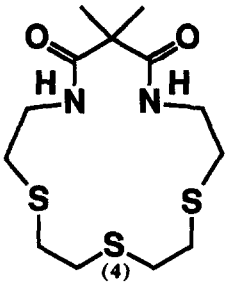

($\nu_{C=O}$ 1647 cm^{-1})

14

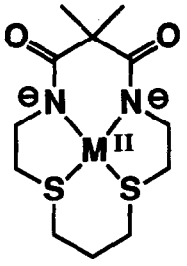

15a M = Pt ($\nu_{C=O}$ 1610 cm^{-1})

15b Pd ($\nu_{C=O}$ 1595 cm^{-1})

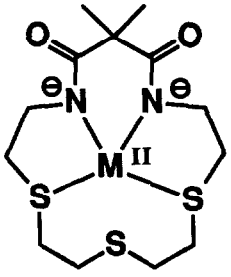

16a M = Pt ($\nu_{C=O}$ 1586, 1599 cm^{-1})

16b Pd ($\nu_{C=O}$ 1559, 1582 cm^{-1})

The amide-deprotonated structures **15** and **16** were established by the similarity in their IR ($\nu_{C=O}$) and UV (L→M CT transition) spectral behaviors to those of the above mentioned dioxocyclam complexes **11**. Pt^{II} complex of the S_3 ligand **16a** possesses a four-coordinated, square planar geometry with $(N^-)_2S_2$, where the central S(4) atom is not coordinated, as shown by the X-ray crystal structure.[26]

Mechanistically and (probably) medicinally more interesting with these new dioxocyclams are that they can remove Pt^{II} from cisplatin (*cis*-$[Pt^{II}(NH_3)_2Cl_2]$) much more efficiently and rapidly than dioxocyclam does to yield the "Pt^{II}-in" complexes **15a** and **16a** without any external additives (Figure 10). The isolation yields of the "Pt^{II}-in" complexes are 40 % for the S_2 ligand **15a**, 38 % for the S_3 ligand **16a**, and below ~1% for dioxocyclam **17** in CH_3OH/HEPES buffer (pH 7) in the presence of equivalent cisplatin at 35 °C for 24 h.

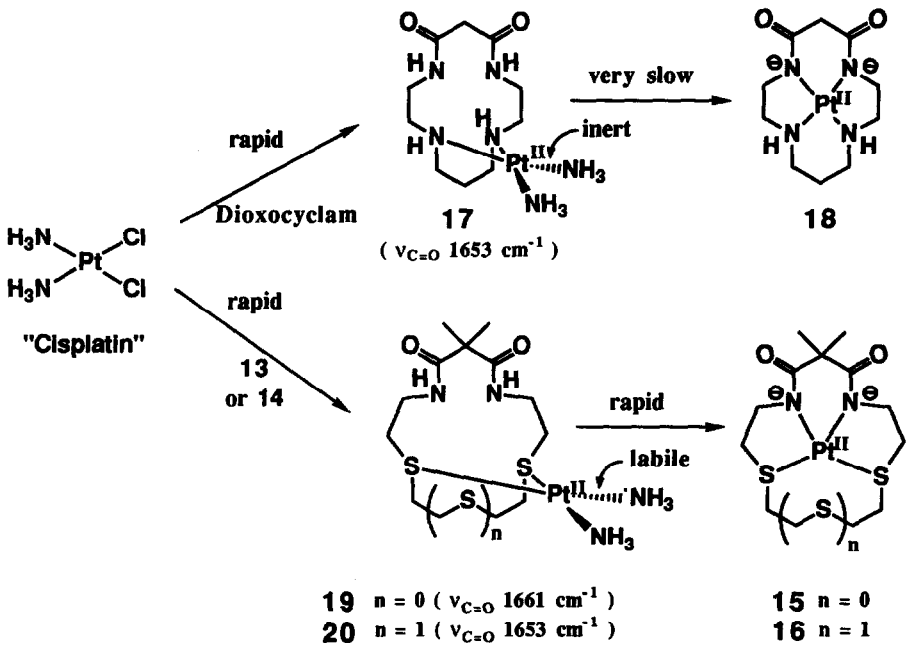

Figure 10. Reaction routes of Pt^{II} uptake from cisplatin by different dioxocycalms

The labile chloride ions in cisplatin are first attacked by the initially available NH and S donors to give intermediates **17**, **19**, and **20**, respectively, which were independently isolated and characterized.[26] In the N_4 complex **17**, the Pt-NH_3 bondings are inert and hardly proceed to the final "Pt-in" complex **18**. In the contrast, the Pt-NH_3 in the S_2 **19** or S_3 **20** complex are labile under the trans effect of the two S donors.

The significance of the amide function as a precursor of the N^- donor is well demonstrated by the reactions of the (amide-reduced) N_2S_2 cyclam **21** for the indiscriminate uptake of all of the divalent metal ions to **22** (Figure 11) and by the failure of Pt^{II}-extraction from cisplatin.

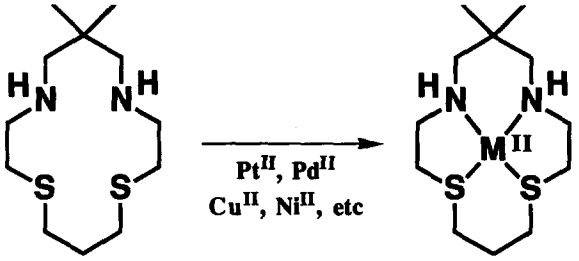

21 22

Figure 11.

2.3. *Selective Gold(III) Uptake with Cyclam 1*

The first Au^{III}-cyclam complexes were recently synthesized and characterized.[29]

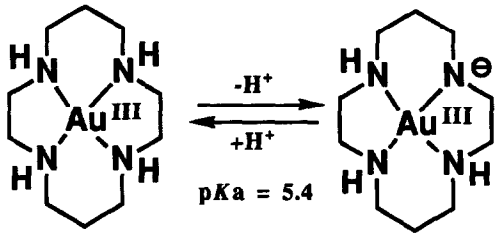

"Au^{III}-in" complex

23 24

Figure 12. Dissociation of a proton from Au^{III}-cyclam 23

The pH titration of Au^{III}-cyclam **23** with 0.1 M NaOH showed removal of a proton with p*K*a value of 5.4 at 25 °C, I = 0.1 ($NaClO_4$), which is assigned to the deprotonation from one of the secondary amines to **24** (Figure 12). The dissociation of a proton from the cyclam NH with such a low p*K*a value has never been observed with divalent metal ions. An X-ray crystal analysis of Au^{III}-cyclam **23** showed a square planar structure with the most stable "trans-III" configuration of cyclam and an average Au-N bond distance of 2.02 Å.[30]

Mixing cyclam with $NaAu^{III}Cl_4$ in aqueous 1 M HCl solution immediately precipitated a yellow "Au^{III}-out" diamino complex **25** in quantitative yield. It is to be noted that under such acidic conditions other divalent metal ions can hardly interact with cyclam. At appropriate pH~3 the "Au^{III}-out" cyclam complex **25** dissociates Au (either as Au^{III} or oxide forms *etc*, exact Au forms are unidentified yet), instead of Au^{III} going into the cyclam cavity (to the "Au^{III}-

in" complex **23**) (Figure 13). This is probably due to hydrolysis of Au^{III}-Cl, whose products (*e.g.* Au^{III} oxides) are extremely stable and no longer sequestered by cyclam.

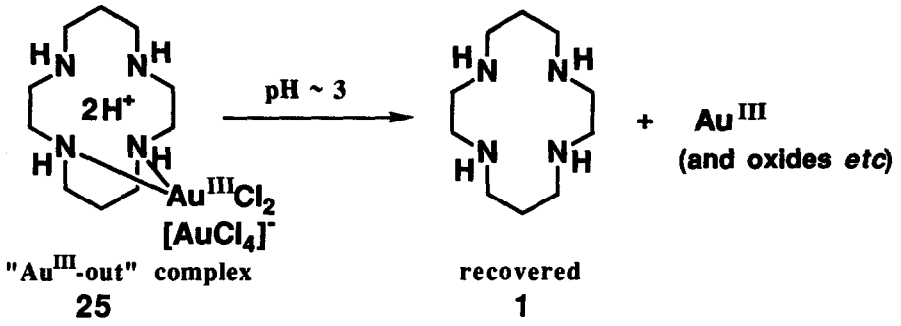

Figure 13. Dissociation of Au^{III} form "Au^{III}-out" complex

Accordingly, the selective solvent extraction of Au^{III} was tested by using lipophilic cyclams **12**, **26** and **27** (Figure 14).[29] The procedure is as follows ; 5 mL of 1.0 mM $NaAuCl_4$ with or without a mixture of the same amount of Cu^{II}, Fe^{III}, Co^{II} and Pd^{II} in an aqueous 1M HCl solution was well stirred with 5 mL of 2.0 mM a lipophilic cyclam ligand in $CHCl_3$ at 25 °C for 30 min. The remaining [Au^{III}] in the 1 M HCl (aqueous layer I) was measured by an atomic absorption spectrophotometer. Then, the Au^{III}-containing (possibly as complexes like **25**) $CHCl_3$ layer was reextracted with 5mL of distilled water (aqueous layer II) at 60 °C for 30 min, which was then assayed for Au^{III}. The results are summarized in Table I. An important principle here is to take full advantage of the acidic properties of Au^{III} being the strongest among the competing metal ions to beat protons which are the most powerful blocking agent for uptake of metal ions by cyclam.

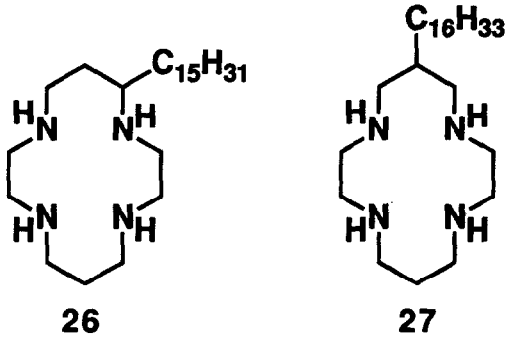

Figure 14. Lipophilic cyclams for solvent extraction of Au^{III}

Table I. Solvent-extraction of Au(III) with lipophilic cyclams 26, 27, and 12 in $CHCl_3$.[29]

run	ligand in $CHCl_3$ layer	metal ions[a] in *aq.* layer I	[Au] remaining[b] in *aq.* layer I, %	[Au] extracted[b] into *aq.* layer II, %
1	none	Au^{III}	100	0
2	none	Au^{III}, Cu^{II} etc.[c]	100	0
3	**26**	Au^{III}	6	81
4	**26**	Au^{III}, Cu^{II} etc.[c]	22[d]	67
5	**27**	Au^{III}	16	65
6	**27**	Au^{III}, Cu^{II} etc.[c]	25[e]	61
7	**12**	Au^{III}	85	9
8	**12**	Au^{III}, Cu^{II} etc.[c]	99[f]	1
9	*n*-$C_{16}H_{33}NH_2$	Au^{III}	50	38
10	*n*-$C_{16}H_{33}NH_2$	Au^{III}, Cu^{II} etc.[c]	42[g]	25

[a] In 1M HCl aqueous solution. [b] All the values have errors within ±5 %. [c] 1.0 mM each of Au^{III}, Cu^{II}, Fe^{III}, Co^{II}, and Pd^{II} ions were contained in 1 M HCl aqueous solution. [d] Other remaining metal ions are $[Pd^{II}]$ = 83 %, $[Fe^{III}]$ = 99 %, $[Cu^{II}]$ = $[Co^{II}]$ = 100 %. [e] Other remaining metal ions are $[Pd^{II}]$ = 46 %, $[Fe^{III}]$ = 99 %, $[Cu^{II}]$ = $[Co^{II}]$ = 100 %. [f] Other remaining metal ions are $[Pd^{II}]$ = $[Fe^{III}]$ = $[Cu^{II}]$ = $[Co^{II}]$ = 100 %. [g] Other remaining metal ions are $[Pd^{II}]$ = 51 %, $[Fe^{III}]$ = $[Cu^{II}]$ = $[Co^{II}]$ = 100 %.

2.4. *A New Mg^{2+} Ion Receptor*[31]

Intraannular phenol-containing macrocyclic polyamines **28** and **29** were found to possess novel uptake features for alkaline earth metal ions.[31]

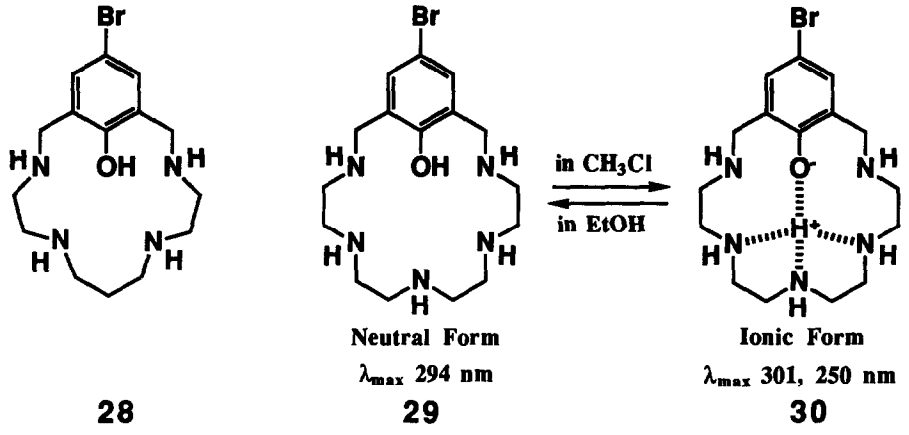

Figure 15. Self-dissociation of intraannular phenol-containing macrocyclic polyamines

Due to the extremely strong basicities (see Introduction), the azacrown rings here are efficient acceptors from the intraannular phenol. Both the neutral phenol **29** (λmax 294 nm) and ionic phenoxide **30** absorptions (λ_{max} 301 and 250 nm) are coexistent in the electronic spectra of **28** and **29** in anhydrous EtOH and $CHCl_3$ (Figure 15). The pentaamine **29** is almost in 1 : 1 metal-ionic ratio in EtOH and 1 : 0.75 in $CHCl_3$. The phenol ionization in EtOH is further promoted by addition of neutral alkaline earth salts, $MgCl_2$, $CaCl_2$, $SrCl_2$, or $Ba(SCN)_2$ (Figure 16).

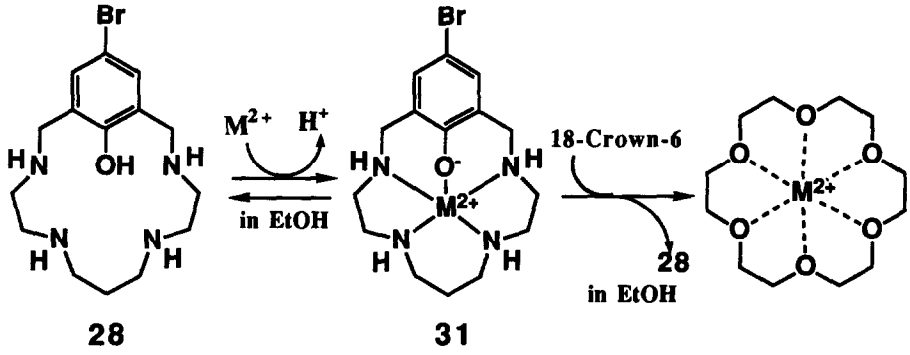

Figure 16. Alkaline earth metal ion inclusion into the intraannular phenol-containing macrocyclic polyamines and competition with 18-crown-6

The apparent 1 : 1 complexation constants K (= [M^{2+}-complex] / [M^{2+}] [$H_{-1}L$], M^{-1}) in EtOH are determined (Table II). As the M^{2+} size increases, complexation becomes more favorable with the larger macrocyclic ligand **29**. This size effect suggests that the metal inclusion into the size-fitting polyamine cavity is a determining factor for the selective uptake.

Table II. 1 : 1 Metal complexation constants for 28 and 29 (log K)

metal ion (ion diameter, Å)	**28**[a,c]	**29**[a,d]	15-crown-5[b,e]	18-crown-6[b,f]
Mg^{2+} (1.30)	3.3	3.1	noncomplxtn	unreported
Ca^{2+} (1.98)	2.9	2.9	2.1	3.9
Sr^{2+} (2.26)	2.3	2.6	2.6	>5.5
Ba^{2+} (2.70)	1.6	2.4	unreported	7.0

[a] K = [M^{2+}-complex]/[M^{2+}][$H_{-1}L$] (M^{-1}) in EtOH at 25 °C. Standard deviation is ±0.1. [b] K = [M^{2+}-complex]/[M^{2+}][$H_{-1}L$] (M^{-1}) in MeOH at 25 °C (ref 32). [c] Cavity Size (1.4-2.0 Å). [d] Cavity Size (1.8-2.2 Å).[e] Cavity Size (1.7-2.2 Å). [f] Cavity Size (2.6-3.2 Å).

Furthermore, in EtOH the complexation of Mg^{2+} and Ca^{2+} with **28** or **29** is stronger than with 15-crown-5 or 18-crown-6, while that of Sr^{2+} and Ba^{2+} with **28** or **29** is weaker than with 18-crown-6. This was revealed by the change of the phenolate UV absorptions upon addition of 1 equiv. crown ethers to a 1 : 1 mixture of **28** (or **29**) and MX_2 in EtOH (Figure 16).

3. Macrocyclic Polyamines for Catalysts and Enzyme Models

3.1. *The Unusual O_2-Uptake and Activation by Ni(II) in New Macrocyclic Dioxopentaamines*

A newly synthesized dioxo[16]aneN$_5$ **32** forms a 1 : 1 square pyramidal complex **33** with high-spin Ni^{II}, which possesses two deprotonated amide donors at equatorial positions (Figure 17).[33]

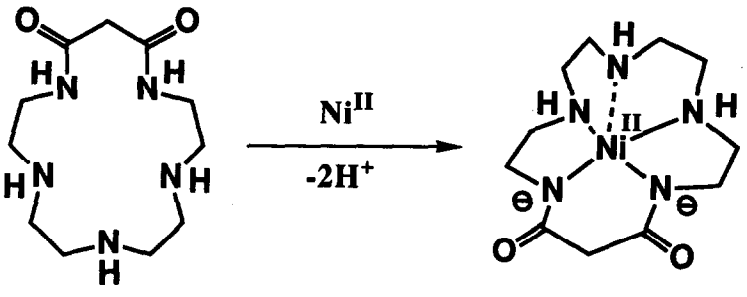

32
Dioxo[16]aneN$_5$

33
high-spin
square-pyramidal
$E_{1/2}$ = +0.24 V
(for Ni$^{III/II}$)

Figure 17.

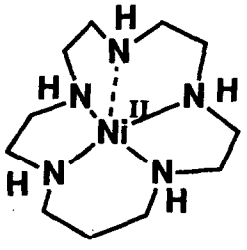

34
high-spin
square-pyramidal
$E_{1/2}$ = +0.66 V
(for Ni$^{III/II}$)

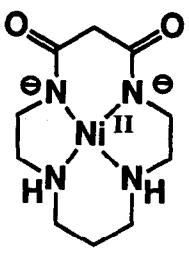

35
low-spin
square-planar
$E_{1/2}$ = +0.81 V
(for Ni$^{III/II}$)

While Ni^{II}(low-spin)-dioxocyclam complex **35** has $E_{1/2}$ of +0.81 V (*vs* SCE) and Ni^{II}(high-spin)-[16]aneN$_5$ complex **34** +0.66 V for Ni^{III}/Ni^{II} couple, the Ni^{II}-dioxo[16]aneN$_5$ complex **33** that combines those functionalities shows an abnormally low $E_{1/2}$ value of +0.24 V under the same conditions in aqueous solution.[33] This is the lowest $E_{1/2}$ value reported for Ni^{III} / Ni^{II} couple in macrocyclic polyamine complex in aqueous solution, which suggests the

easiest $Ni^{II} \rightarrow Ni^{III}$ oxidation and the stability of the Ni^{III} species. An X-ray crystal structure of the Ni^{II} complex **33** confirmed the square-pyramidal geometry,[34] as depicted in Figure 18. The steric strain for the (relatively large sized) high-spin-Ni^{II} ion suffering from the tight macrocyclic cavity is evident from (1) the distorted square pyramidal, (2) the Ni^{II} ion lying 0.22 Å from the basal plane toward the apical N, and (3) the apical Ni-N bond bent by 18.4° from perpendicular. This steric factor partially contributes to the observed extremely low $Ni^{I} \rightarrow Ni^{II}$ oxidation potential.

Indeed, air oxidation yielded the brown-colored Ni^{III} complex, an uncommon observation for Ni^{II}-polyamine complexes. The crystal structure of the Ni^{III} complex **36** has proven less steric strain with a more ideal square-pyramid structure.[35] Hence, we conclude that reduction of the steric strain plays an important role in lowering the $E_{1/2}$ value for $Ni^{III/II}$ in the dioxo[16]aneN$_5$ complexes. It is of interest that the $E_{1/2}$ values for $Cu^{III/II}$ with dioxocyclam (+ 0.64 V) and dioxo[16]aneN$_5$ (+ 0.68 V) are almost the same.[36]

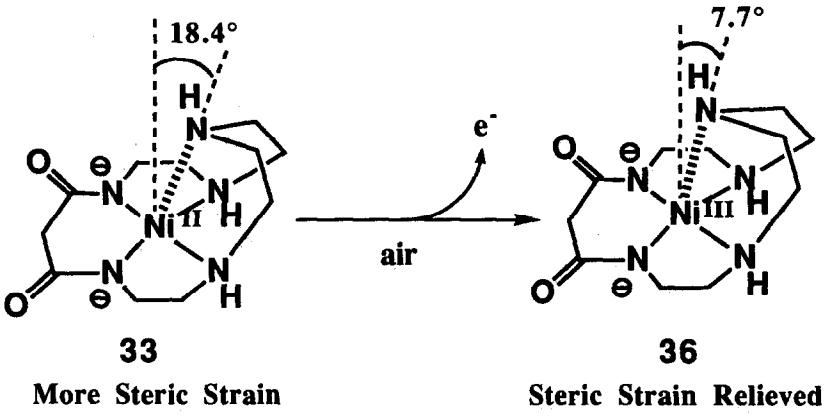

Figure 18. Square pyramidal configurations for high-spin Ni^{II} and low-spin Ni^{III}

Most interesting of all with the Ni^{II}-dioxo[16]aneN$_5$ complex is that at room temperature it binds with O_2 to a 1 : 1 adduct **37** in aqueous solution,[36,37] and by doing so, it activates O_2, which reacts with benzene to yield phenol, where the phenol oxygen derives 100% from O_2 and not from H_2O (Figure 19).[37]

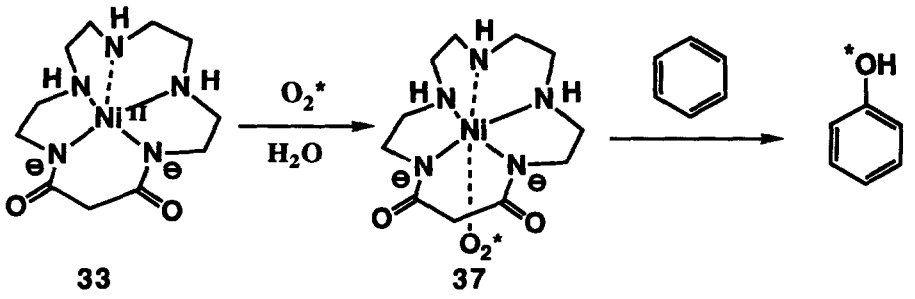

33 37

Figure 19. Interaction of O_2 with 33 for a monooxygenase-like reaction

Two interesting research themes would emerge. One is the mechanistic studies of this novel Ni-O_2 activation, which may or may not be relevant to the reactions of monooxygenases such as cytochrome P450. Another would be applications as a catalyst for direct synthesis of phenols from benzene (or substituted benzene) and O_2 at room temperature and atmospheric pressure.

3.2. Zinc(II)- Macrocyclic Polyamine Complexes as Zinc-enzyme Models

Numerous Zn^{II}-containing enzymes are known. Metalloenzymes that are involved in hydrolysis of carboxylic esters, amides or peptides, phosphates, and hydration of biological molecules almost exclusively contain Zn^{II} ion at the active center.[38,39] Then, questions naturally occur: why nature picks up zinc(II) among dozens of metal ions? or what are their special properties pertaining to their biological functions? Prof. Bertini summarizes the particular properties of zinc(II) from his numerous studies of zinc-enzymes as follows:[40] (1) zinc(II) can be easily tetra-, penta-, or hexa-coordinated, without a special preference for the latter geometry. Zinc enzymes usually have coordination numbers fewer than six so that they have open reactive sites. Take carbonic anhydrases (CA), where zinc is surrounded by three imidazoles and a water in a distorted tetrahedron (Figure 20). The substrates (*e.g.* HCO_3^-) can bind with zinc(II) by substituting for the coordinated water or by increasing the coordination number to five (trigonal bipyramid). (2) the zinc(II) bound H_2O in zinc enzyme catalytic site has a p*K*a value of ~7 appreciably lower than that of free water (15.5), so that significant concentration of Zn^{II}-OH^- species exists at physiological pH. The coordinated hydroxide

appears to function as a good nucleophile for electrophilic centers such as carbonyl carbons in esters, amides, or CO_2. The pKa of the zinc(II)-binding H_2O is controlled by the total coordination number and by the total charge of the complexes. The pKa values are further controlled by the presence of (±) charged groups and anions bound to zinc(II). And (3) zinc(II) complexes have little kinetic barrier between the 4- and 5-coordination interaction.

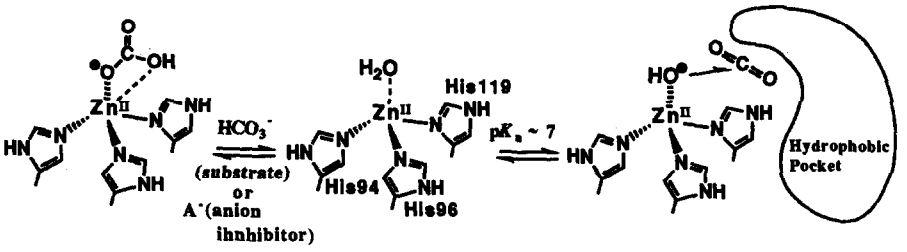

Figure 20. Reactions involved at active center of carbonic anhydrase

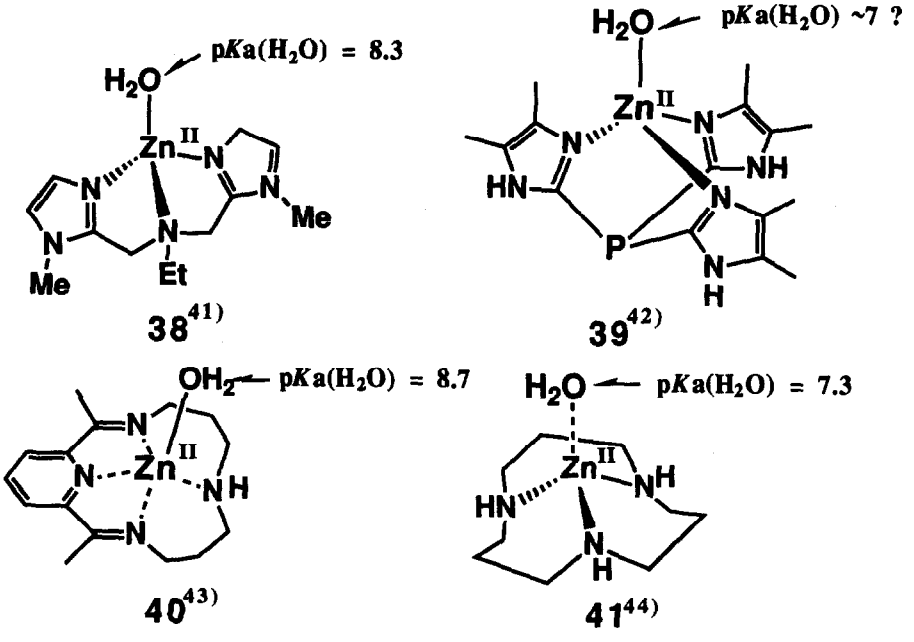

Figure 21. Various models for carbonic anhydrase active center

Direct spectroscopic investigation of zinc enzymes poses difficulty because Zn^{II} (d^{10}) is colorless and diamagnetic, and cannot be studied through electronic or ESR spectroscopy, etc. The enzymes have been mostly studied by substituting Zn^{II} with other spectroscopically "visible" metal ions (*e.g.* Cd^{II}, Mn^{II}, Co^{II}, Cu^{II}, etc.). Another approach to elucidate the role of metal ion in zinc enzymes would be construction of model complexes that have the similar structure and functions. However, a few models with small Zn^{II} complexes had been successful in elucidating the functions of Zn^{II}, as Prof. Bertini characterized (for CA models, see Figure 21). The main reasons lie in a lack of ligands that could provide appropriate structural environments similar to those of enzymes and at the same time that can function like enzymes so as to permit defining the biological suitable nature of Zn^{II} ion. Because of scarce experimental facts about the inherent properties of Zn^{II}, some of the chemical feasibility of the conclusions or propositions derived from enzymological studies on the functions of Zn^{II} had remained to be verified. To cite a few instances, while the p*K*a value of ~7 had been assigned to deprotonation of the water bound to Zn^{II} in CA (Figure 20), there was no Zn^{II} complex known that has a dissociable H_2O with p*K*a as low as ~7.5 until **41** was constructed (Figure 21). Or, while anion (*e.g.* SCN^-, I^-, etc.) inhibition of CA activities had been explained by occupation of the H_2O binding site, there had been no chemical analogy with the past zinc complexes.

Lately, new Zn^{II} complexes with three-coordinate ligands (*e.g.* **38**, **39**) have been constructed as models for CA independently by several groups. Although they looked structurally well mimicking CA, the frequent insolubility in H_2O (*e.g.* **39**) or lack of complex stability in aqueous solution prevented ones from studying deep insight into the roles and functions of Zn^{II}.

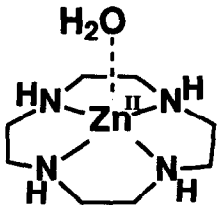

42

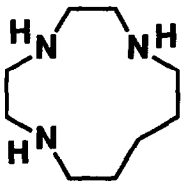

43

Macrocyclic polyamine ligands are quite advantageous in constructing Zn^{II} coordination environments in zinc enzymes because of the enormous complex stability (as mentioned in Introduction) that would allow otherwise unstable Zn^{II} complex to be formed, due to the "macrocyclic effects". Note that Zn^{II}-amine complexes in general are not as stable as non-d^{10} transition metal ion complexes.

In 1975, the macrocyclic tetraamine Zn^{II} complex **40** was introduced as a CA model by Woolley.[43] This model drew intriguing and well-illustrating pictures about the kinetic function of Zn^{II} ions. However, the drawbacks were its Zn^{II} coordinate structure being N_4 coordinated (against N_3 coordination in CA) and as a result the higher p*K*a value of the bound H_2O being 8.7 (against ~7.5 in CA). This study did not provide the well-known thermodynamic role of Zn^{II} such as anion and neutral sulfonamide inhibition of CA. Since then, Zn^{II}-cyclen **42**[45] and Woolley's tetraamine[46] and its modified complexes[47] had been tested as another zinc enzyme, phosphatase model. Again, most of these model studies had been concerned chiefly with kinetic aspects (*i.e.* the major emphases were hydrolysis rate enhancements) towards substrates, while they paid less attention to the equilibrium aspects.

Recently, we have discovered that a macrocyclic triamine [12]aneN$_3$ complex of Zn^{II} **41** can reproduce the simplest and yet the closest environment known so far of the active metal center of CA, which has given the best structural and functional mimic.[44] A number of scattering biochemical phenomena possibly arisen from the active metal could be correlated through the new knowledge about **41** coordination chemistry.

First, let us look at how the N chelation influences the Zn^{II} acidity that promotes the proton dissociation from Zn^{II}-OH_2. Zinc(II) complexes of various macrocyclic triamines and tetraamines were potentiometrically measured for 1 : 1 complexation constants and at the same time for p*K*a values of Zn^{II}-OH_2 in the macrocyclic complexes. The most interesting finding was that N_3 ligands, [12]aneN$_3$ **2** and iso[12]aneN$_3$ **43** yield 4-coordinate, tetrahedral complexes, wherein Zn^{II}-OH^- was readily generated with p*K*a value of 7.3. Although we must await theoretical treatments to explain why these N_3 ligands caused the Zn^{II} ions to be so acidic, the observed p*K*a of 7.3 is almost comparable to that reported for CA. These macrocyclic triamine complexes seemed to offer an ideal model to test the reactivity of the common Zn^{II}-OH^- species with that of CA. It is noteworthy that if triamines are

nonmacrocyclic (*e.g.* diethylenetriamine), the Zn^{II}-N_3 complexes are much less stable, appreciable decomplexation are occurring at physiological pH, and hence well-defined Zn^{II}-OH^- species are difficult to generate from them.

3.2.1. *Strong Affinities of Anions to Zn^{II}-Macrocyclic Polyamine Complexes and CA*

The pH-metric titration for 1 : 1 Zn^{II}-[12]aneN$_3$ in the presence of excess anions A^-, (AcO^-, SCN^-, I^-, Br^-, Cl^-, F^-) immediately disclosed some interaction between the Zn^{II} complex and A^-.[44] The calculation results for the 1 : 1 A^--Zn^{II}-[12]aneN$_3$ **44** complexation constants were compared with the reported K_i values obtained kinetically for CA (Table 3). It was a great surprise that the *order and magnitude of these 1 : 1 anion association constants are very similar for our model* ***41*** *and CA*. On the other hand, comparing the halogen anion affinities, *we see the opposite behaviors between the Zn^{II} complex* ***41*** *and Zn^{II}_{aq}*. The discrepancy in the Zn^{II} associations with halogen anions between CA (reported by biochemists) and Zn^{II}_{aq} (reported by chemists) had been quite puzzling and hence, there had been unbridgeable gap between the CA chemistry and Zn chemistry. For the first time from chemistry side, we could contribute to the biochemical conclusion that these inhibitor anions A^- are indeed intimately binding (*i.e.* coordinating) to Zn^{II} at the active center of CA, as modeled by **44**.

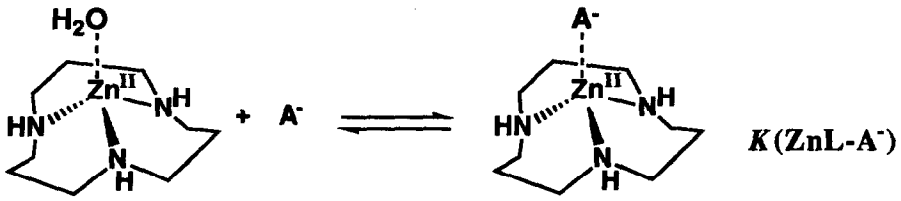

41 **44**

Table III. 1 : 1 Anion association constants log K(ZnL-A$^-$) at 25 °C with model complexes 41 and CA[a]

anion	41	Zn^{II}-CA[b]	Zn^{II}_{aq}[c]	42
OH^-	6.4	6.5	5.0	6.0
CH_3COO^-	2.6	1.1	0.9	1.7
SCN^-	2.4	3.2	0.7	2.1
I^-	1.6	1.2	-1.5	1.0
Br^-	1.5	1.1	-0.6	1.0
Cl^-	1.3	0.7	0.1	1.3
F^-	0.8	-0.1	0.8	0.7
$HCO3^-$		1.6	0.3	

[a] $K(A^-)$ = [complex-A^-]/[complex][A^-] (M^{-1}). [b] Calculated values using inhibition activities of bovine CA in 4-nitrophenyl acetate hydrolysis (ref 48) [c] At 25°C (ref 13.)

Interestingly, a potential bidentate anion $CH_3CO_2^-$ has higher affinity than halogens to Zn^{II}-[12]aneN_3 complex **41**, a fact suggesting the possible availability of more than one coordination site on the Zn^{II}-N_3 complex. As if supporting this explanation, with a Zn^{II}-N_4 (cyclen) complex **42** the anion affinity trend changes; *i.e.* binding of $CH_3CO_2^-$, I^-, and Br^- decreases. This fact seems to imply that the Zn^{II}-N_3 complex has more open space for the (potential) bidentate $CH_3CO_2^-$ or bigger sized halogen donors, whereas the Zn^{II}-N_4 complex has less vacant site to allow only monodentate and smaller anion bindings.[49] A four coordinate, tetrahedral Br^--Zn^{II}-[12]aneN_3 complex **45** had been isolated and its X-ray crystal structure was reported.[50] Recently, we have obtained a five coordinate, trigonal bipyramidal $(SCN^-)_2$-Zn^{II}-[12]aneN_3 complex **46**, which was characterized by X-ray crystal analysis.[51] This is a good chemical verification of the biochemical postulate that four-coordinate, tetrahedral ⇌ five-coordinate, trigonal-bipyramidal equilibrium can be intrinsically taken by

different ligands. The equatorial Zn^{II}-NCS$^-$ bond is shorter (2.012 Å) and the apical Zn^{II}-NCS$^-$ bond longer (2.119 Å). In poorly defined X-ray analysis of the SCN$^-$-bound CA, the Zn^{II} ion seems to take a five coordinate geometry with an equatorial SCN$^-$ and an apical H_2O.[52] In our model study, despite we started from the symmetrical (*i. e.* tetrahedral) H_2O-Zn^{II}-[12]aneN$_3$ **41**, two SCN$^-$ coordinations become unequivalent. This fact implies an intrinsic property of Zn^{II} ion that can go to five-coordinate, trigonal bipyramidal structure, as Prof. Bertini noted.[40]

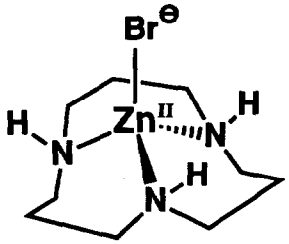

45

Tetrahedral Four-Coordinate

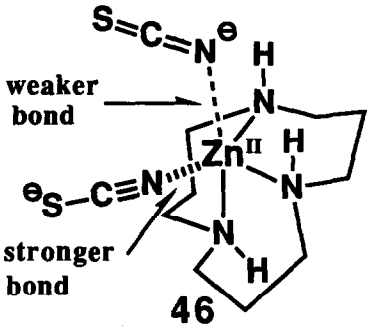

46

Trigonal Bipyramidal Five-Coordinate

Very recently, we have proven strong affinity of a CA substrate HCO_3^- anion to Zn^{II}-[12]aneN$_3$ **41** by kinetic inhibition of *p*-nitrophenylacetate ester hydrolysis promoted by HO$^-$-Zn^{II}-[12]aneN$_3$ (see below).[53] The log *K* value of HCO_3^- is greater than for ordinary anion bindings (*e.g.* Cl$^-$, see Table III). Although our value is deviated from the reported value (1.6) for CA, HCO_3^- affinity commonly seems greater with respect to halogen anions. Thus, our model appears to repeat the intrinsic roles Zn^{II} in CA. Our model data for the order in Zn^{II}-A$^-$ affinities are very instructive in the accounting for a previous enzymological observation that at high pH (>9), the anion inhibition is abolished. Thus, it explains that with the p*K*a value being 7.3 for generation of Zn^{II}-OH$^-$ (or log *K* value is a far higher value of 6.7 than those for other A$^-$, Table III), inhibitor anions are unlikely to displace OH$^-$ at alkaline pH. Furthermore, we could argue that for a substrate HCO_3^- interaction with Zn^{II} (for dehydration to CO_2+OH$^-$), the Zn^{II}-OH$^-$ species must be converted to Zn^{II}-OH_2 species, which can (thermodynamically speaking) be easily done by slightly lowering pH to a bit acidic side. However, for the reverse

CO_2 hydration to occur the Zn^{II}-OH^- species must be restored at a little basic pH side. For both the forward and backward reactions properly to occur, the thermodynamically most useful media pH should be adjusted to the p*K*a value for the Zn^{II}-$OH_2 \rightleftharpoons Zn^{II}$-$OH^-$, which is exactly the case in our body; *e.g.* blood pH is set at ~ 7 !! (see Figure 22).

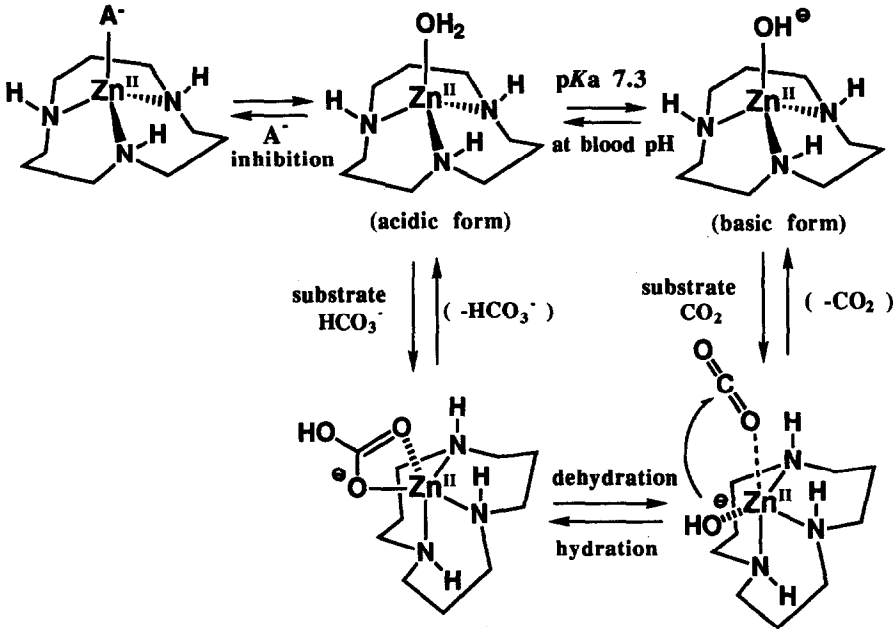

Figure 22. Illustration of anion A^- inhibitors, OH_2, OH^-, HCO_3^- substrate and CO_2 binding to Zn^{II} on the basis of our model study

3.2.2. *Why Neutral Sulfonamides, phenol and imidazole are Strong Inhibitors of CA*

The inhibition of CA activities by neutral aromatic sulfonamide (*e.g.* acetazolamide which is actually used as a diuretic drug) had been extensively studied and now it is accounted for by direct interaction of the sulfonamide anion ($ArSO_2NH^-$) with Zn^{II} at the active center. The X-ray crystal analysis of the CA-acetazolamide complex (to 2.0 Å resolution) appears to confirm this explanation (Figure 23).[52] For coordination chemists this was somewhat puzzling, because transition metal ions (*e.g.* Ni^{II}) would be expected to bind with acetazolamide rather *via* the thiazole N than *via* the deprotonated N^-.[54] There was no chemical confirmation for this

enzymological explanation about the sulfonamide inhibition mechanism. The question was thus whether Zn^{II} intrinsically displaces the amide hydrogen to bind with the resulting sulfonamide anion at physiological pH. Note the aromatic sulfonamides have p*K*a values of ~10. Unless Zn^{II} especially favors $ArSO_2NH^-$ as a coordinate partner, this dissociation would not occur at pH ~7.

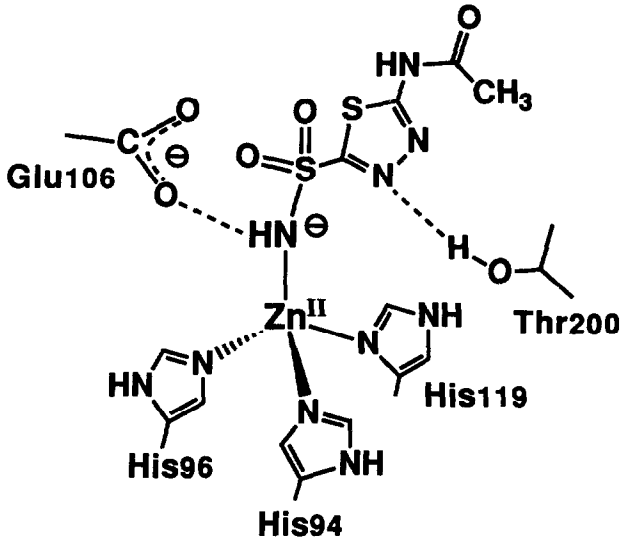

Figure 23. X-ray structure of CA and acetazolamide (as an anion) interaction

Treatment of acetazolamide with Zn^{II}-[12]aneN$_3$ **41** in acetonitrile immediately yielded a microcrystalline product, which was characterized as a 1 : 1 ternary complex **47** wherein the sulfonamide nitrogen is deprotonated.[44] Thus, *the outstanding acid character of Zn^{II} in the N_3 coordinating environment that favors anionic N$^-$ donors over the heteroaromatic donors is first demonstrated.* The p*K*a value of 7.42 (25 °C, I = 0.1) for the sulfonamide of acetazolamide is close to that for the Zn^{II}-OH_2 (p*K*a = 7.3). Thus, the easy deprotonation of sulfonamides with simultaneous coordination would be facilitated.

The other neutral sulfonamides *p*-nitrobenzenesulfonamide (p*K*a = 9.4), and *p*-toluenesulfonamide (p*K*a = 10.5) and the anionic substrate HCO_3^- were also kinetically proven to inhibit the catalytic activity of OH^--Zn^{II}-[12]aneN$_3$ in the carboxylic ester hydrolysis (Rx

1).[53] From the order of the inhibition the 1 : 1 binding constants K_i were determined using the Dickson-like plot ($1/v = K_i[I]/v_{max}+1/v_{max}$) (Table 4).[53] Our model results of log Ki are parallel to the reported log K_i for CA, implying that our chemical model well illustrates the biochemical CA inhibition mechanism.

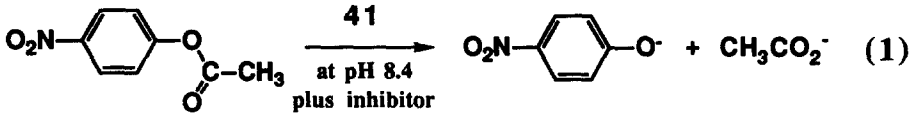

(1)

Table IV. Comparison of neutral and anion inhibitors affinity constants with Zn^{II} 41 and with CA

	41		CA	
Inhibitor	log K_i [a]	log $K(Zn^{II}L\text{-}I^-)$	log K_i [c]	
acetazolamide	3.6 ± 0.1	4.9 [a]	6.7 [d]	7.9 [e]
4-nitrobenzenesulfonamide	2.6 ± 0.1	4.8 [a]		7.2 [e]
p-toluenesulfonamide	2.4 ± 0.1	5.7 [a]		6.3 [e]
HCO_3^-	2.8 ± 0.1	4.0 [a]	1.6 [d]	
CH_3COO^-		2.6 [b]	1.1 [d]	
SCN^-		2.4 [b]	3.2 [d]	
Cl^-		1.3 [b]	0.7 [d]	
OH^-		6.4 [b]	6.5 [d]	

[a] Determined by inhibition kinetics at pH 8.4 (50 mM TAPS buffer), I = 0.10 and 25 °C. K_i = $[Zn^{II}\text{-L-I}]/[\text{inhibitor unbound } Zn^{II}\text{-L}][I]_f$ (M^{-1}). $K(Zn^{II}L\text{-}I^-)$ = [Zn^{II}-L-anionic form of inhibitor$^-$] /[**41**][inhibitor$^-$] (M^{-1}). [b] Determined by potentiometric pH titration at 25 °C and I = 0.10 (ref 44). [c] K_i = $[CA\text{-I}]/[\text{inhibitor unbound CA}][I]_f$ (M^{-1}). [d] Determined by inhibition kinetics in CA-promoted NA hydrolysis at pH 8.5 (Tris buffer) (ref 55). [e] Determined by formation and dissociation kinetics with Human Carbonic Anhydrase at pH 6.5 and 25 °C (ref 56).

An intramolecularly attached tosylamide in tosylamidopropyl-[12]aneN$_3$ **48** has been synthesized to test if the dissociation of the amide proton occurs at pH ~7 in the presence of Zn^{II}.[53] Indeed, dissociation of the amide hydrogen occurs at pH ~ 7 and an anion-bound tetrahedral complex **49** was isolated, which was fully characterized by X-ray crystal analysis. As predicted, this complex **49** has no ester hydrolysis activity.

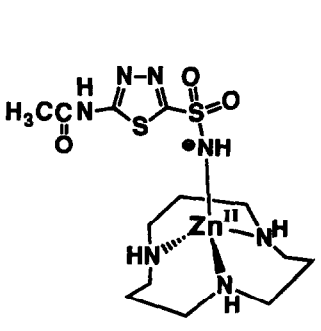

47

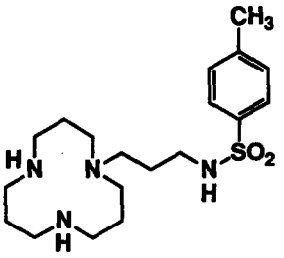

48

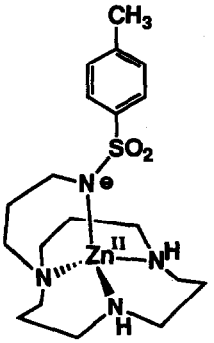

49

Phenol is another inhibitor of CA. A question may be raised if it may also be deprotonated for coordination with Zn^{II}. A possible model for the Zn^{II}-induced deprotonation of a phenol (p*K*a = 6.8, *cf.* ordinary phenol p*K*a ~ 10) was synthesized by another complex **50** of a phenol-pendant [12]aneN$_3$.[57] Its crystal structure[58] is a trigonal bipyramid with an extremely short Zn^{II}-phenolate anion (equatorial) bond distance (1.93 Å). The H_2O apically binds with Zn^{II} at longer distance of 2.22 Å and its p*K*a value of 10.7, a lower value than 7.3 for Zn^{II}-[12]aneN$_3$. As anticipated, this phenolate-binding Zn^{II} complex does not catalyze the ester hydrolysis at all, supporting a notion that the phenolate occupation of the fourth coordination site, like acetazolamide, may likely be responsible for the phenol inhibition of CA.

Imidazole is also an inhibitor of CA. Thus, an intramolecularly attached imidazole to [12]aneN$_3$ was designed.[59] Its Zn^{II} complex **51** is a five-coordinated trigonal bipyramid like **46**. Because the apical H_2O is not so strongly bound to Zn^{II}, its p*K*a is ~ 10.0 and hence, like **49** and **50**, this complex did not catalyze the ester hydrolysis at physiological pH.

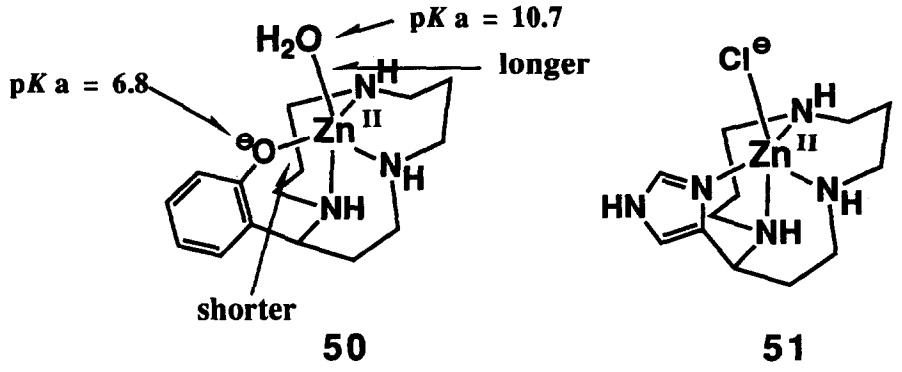

50 51

3.2.3. *The Action of Zn^{II}-OH^- as a Base. Relevance to Carboxyamide Inhibition of CA*

While CA has esterase activities (as we saw in the last paragraph), it has no peptidase activity.[61] It had been suspected that the Zn^{II}-OH^- species in CA probably acts on peptides or amides as a base (rather than as a nucleophile) to produce amide anions that tend to bind with Zn^{II}, resulting in no further amide bond cleavage. Iodoacetamide (CH_2ICONH_2) and ethyl carbamate (NH_2COOEt) were known not to be hydrolyzed but rather known to be CA inhibitors, which were only theoretically proposed to become the amide anions to bind with Zn^{II} in CA,[61] like the previous sulfonamide inhibitors. Unfortunately, we have failed to see the perturbation of ester hydrolysis by ethyl carbonate in the catalytic action of our CA model Zn^{II}-[12]aneN_3 at physiological pH. However, the amide groups included in macrocyclic polyamines are extremely instructive for demonstrating the basic nature of Zn^{II}-OH^-. We illustrate that such macrocyclic ligands can be good chelating agents selective for Zn^{II} against Cd^{II}.[60]

Monooxocyclam **52** ($\nu_{C=O}$ 1670 cm^{-1}) is a good candidate to test if the possible first intermediate N_3-Zn^{II}-OH^- **54** acts a nucleophile (path (a) to **55** in Figure 24) or a base (path (a) to **55**). The result from the pH-metric titration proved that *b* is the exclusive pathway. The product Zn^{II}-inclusion complex **56** was indeed isolated as a perchlorate salt, whose IR spectrum at $\nu_{C=O}$ 1570 cm^{-1} supports the Zn^{II}-binding deprotonated amide structure. Otherwise unfeasible dissociation of carboxyamides (p*K*a ~ 14) should be rendered possible by the Zn^{II}-amide anion bonding in the macrocyclic N_4-coordinate structure. This fact implies the likelihood of the deprotonation and the resulting deprotonated amide coordination of the amide

inhibitors (*e.g.* iodoacetamide, ethylcarbamate) to Zn^{II} in CA, where supplementary interaction of neighboring peptide residues would contribute to stabilizing the anionic amide bondings. By contrast, because of larger size and/or weaker acidity, Cd^{II} can not yield the metal inclusion complex like **56**. Thus, monooxocyclam **52** is the first chelate for distinctively separating Zn^{II} from Cd^{II}.

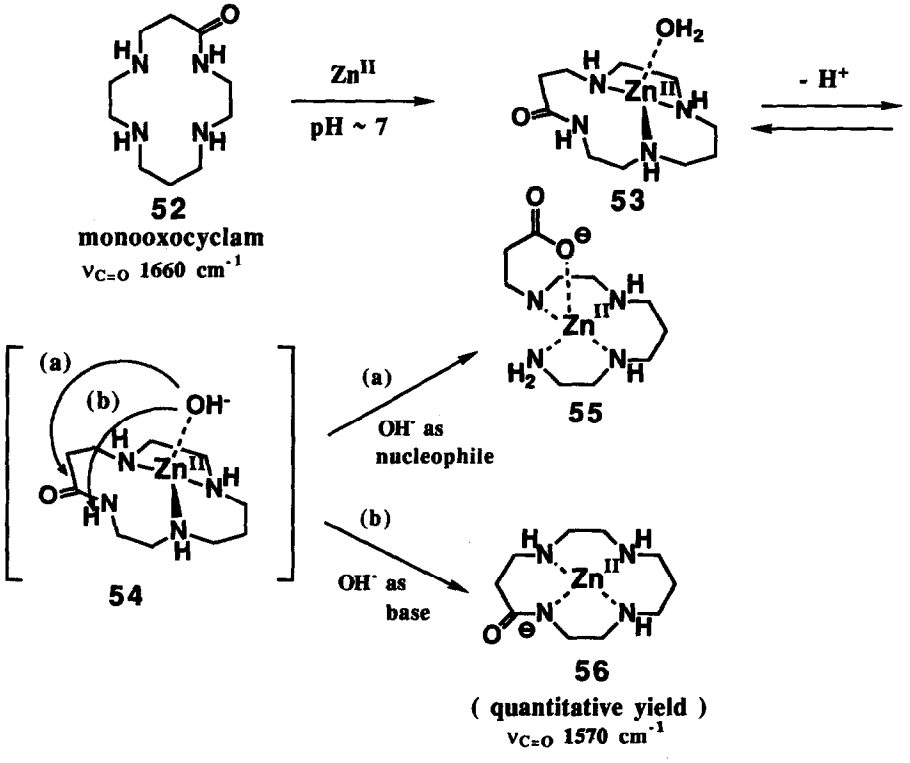

Figure 24. Interaction of monooxocyclam 52 with Zn^{II} at pH ~7

The difference in acidity, size, and coordination characters of Zn^{II} against Cd^{II} is well illustrated by the mode of their interactions with a pyridyl-pendant monooxocyclam at various pH (Figure 25). Zn^{II} binds with three amines and a pyridyl N to yield a four coordinate $[ZnL]^{2+}$ **58** below pH 6, while larger sized Cd^{II} gives a six-coordinate $[CdL]^{2+}$ **60** at higher pH ~7. The X-ray crystal analysis of **60** showed an octahedral structure with additional coordination of an amide oxygen ($\nu_{C=O}$ 1611 cm^{-1}) and a water. Such an expanded six

coordinate Cd^{II} geometry is in contrast to the four coordinate Zn^{II} complex, which is due to the different ion size. The relative acidity (due to the different ion size) of Zn^{II} and Cd^{II} is well demonstrated in the subsequent process of metal-induced amide deprotonation with concomitant metal binding to yield the common $[MH_{-1}L]^+$ **59** and **61**. However, this amide deprotonation occurs at much higher pH for Cd^{II}. The p*K*a for $ML \rightleftharpoons MH_{-1}L$ are 10.6 for Cd^{II} and 7.3 for Zn^{II}. The final amide-deprotonated complex for $[Zn^{II}H_{-1}L]\cdot ClO_4\cdot 3H_2O$ was isolated and characterized by X-ray analysis.

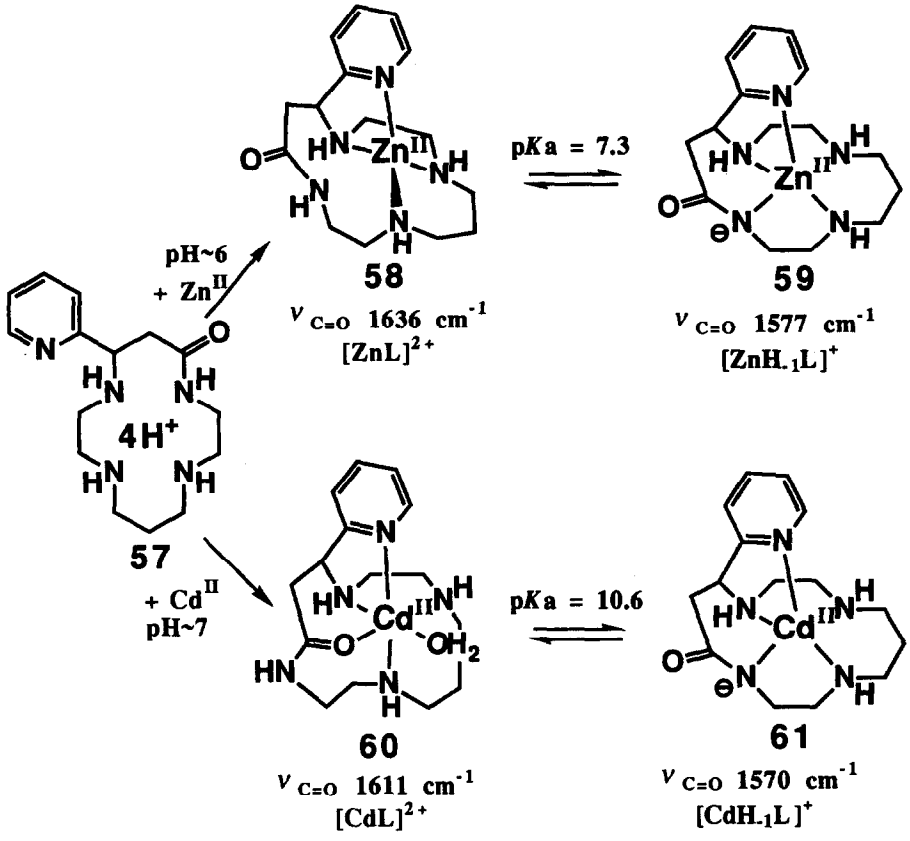

Figure 25. Distinguishing interaction modes of pyridyl-pendant monooxocyclam 57 with Zn^{II} and Cd^{II}

3.2.4. *The Action of Zinc-OH⁻ as a Nucleophile*[62]

In order to assess the nucleophilicity of Zn^{II}-OH^- toward carboxylic esters and phosphate esters, we have measured the hydrolysis rates for acetyl *p*-nitrophenol esters NP, tris(4-nitrophenyl)phosphate TNP^0 (a neutral phosphotriester), and bis(4-nitrophenyl)phosphate, BNP^- (a monoanionic phosphodiester) with HO^--Zn^{II}-[12]aneN$_3$ **41** , HO^--Zn^{II}-[12]aneN$_4$ **42**, and OH^- (Figure 26). The results are summarized in Table V.

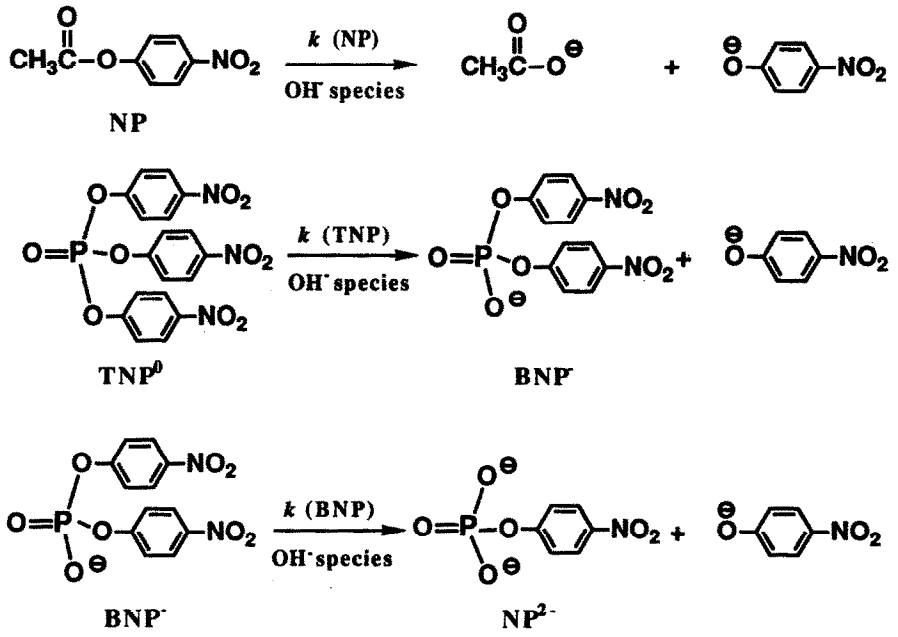

Figure 26. Ester hydrolysis study with various OH^- species

Zn^{II}-[12]aneN$_4$ **42** and Zn^{II}-[12]aneN$_3$ **41** promote the hydrolysis of both phosphates TNP^0 and BNP^-. In the hydrolysis of anionic diester BNP^-, the rates are generally 10^5 times slower than those for the neutral triester TNP^0. This is due to the electrostatic repulsions between the attacking OH^- species and the anionic substrate. When Na^+ (added to keep constant ionic strength in solution) is replaced by Mg^{2+} or Ca^{2+} ion, the BNP^- hydrolysis increases due to the partial neutralization of anionic part of the BNP^- or the (more anionic) reaction transient species (Figure 27). The similar effect is well known in the enzymatic hydrolysis of anionic phosphate (di- or mono-) esters in the presence of Mg^{2+} ion. When Na^+

Table V. Comparison of the second-order rate constants ($M^{-1}sec^{-1}$) for carboxylic ester and phosphate esters with OH^- species

OH^- Species(p*K*a)	*k*(NP)	*k*(TNP)	10^5 *k*(BNP)
OH^-(15.5)	9.5	10.7	2.4
41(7.3)	$1.1x10^{-1}$	3.7	2.1
42(8.0)	$4.1x10^{-2}$	7.0	8.5

is substituted by a bulky tetramethylammonium (Me_4N^+) that cannot closely associate with P-O^- like the smaller and higher charged M^{II} ions, the rate enhancement did not occur. On the other hand, in the hydrolysis of neutral phosphotriester substrate TNP^0, such a rate enhancement effect by the divalent metal ions was not observed, because M^{II} will hardly interact with the neutral phosphate.

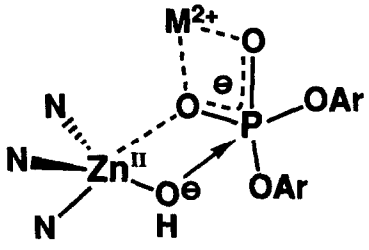

Figure 27. More favorable Zn^{II}-OH^- nucleophilic attack in the presence of M^{II}

From the pH-rate profile in the TNP^0 hydrolysis at 25 °C and the BNP^- hydrolysis at 35 °C (both give a similar sigmoidal curves), the p*K*a values are determined kinetically to be 7.3 and 7.2 for Zn^{II}-[12]aneN_3, and 7.9 and 7.8 for Zn^{II}-[12]aneN_4, which well agree with the p*K*a values determined by the potentiometric pH titrations. Accordingly, it was concluded that OH^--Zn^{II}-[12]aneN_3 and OH^--Zn^{II}-[12]aneN_4 (or their equivalents) are kinetically active

species: *i.e.* these Zn^{II}-OH^- species are indeed nucleophiles. Comparing the relative rate constants of phosphate esters with the previously reported Zn^{II} model complexes,[41,45] we come to conclude that Zn^{II}-[12]aneN$_3$ is probably the best model of Zn^{II}-containing phosphatases in terms of the rate enhancement effects and as a mechanistic probe, as described below.

Two limiting mechanisms may be considered for the phosphate hydrolysis with metal-OH^- species; (Figure 28); (a) an intermolecular nucleophilic attack on the phosphate atom and (b) an activation of the phosphoryl P=O bond by coordination to the electrophilic metal center to become susceptible to external OH^- or OH_2 nucleophilic attack. There is also a "hybrid" mechanism (c) where Zn^{II}-OH^- acts as a nucleophile and at the same time Zn^{II} offers a binding site. These mechanisms might be tested by comparing the hydrolysis rates with Zn^{II}-[12]aneN$_4$ (with less open site) and Zn^{II}-[12]aneN$_3$ (with more open site) for a neutral phosphate triester (TNP^0), an anionic phosphate diester (BNP^-), and a neutral carboxylic ester, 4-nitrophenyl acetate (NP).

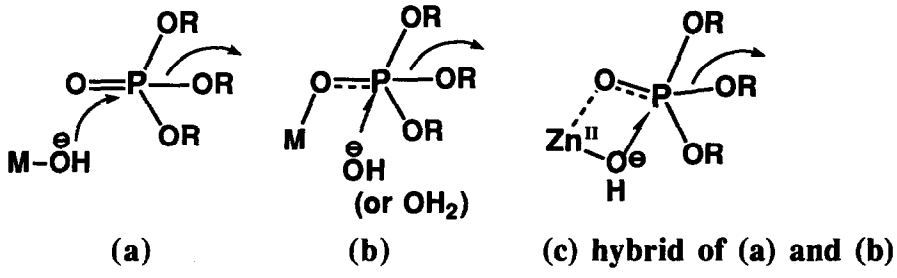

Figure 28. Three possible reaction mechanisms of M-OH^- nucleophilic attack at phosphates

In the carboxylic ester NP hydrolysis, free OH^- ion has a much larger rate constant than those Zn^{II}-OH^- species, where an approximately linear relationship exists between the nucleophilicities (*i.e.* the second order rate constants) of the OH^- species and the basicities (*i.e.* reciprocal p*K*a values, see Table IV). This fact indicates that a simple nucleophilic mechanism is predominant (Figure 29 (a)). In the neutral phosphotriester TNP^0 hydrolysis, although the

reaction of free OH^- species is larger than those of the Zn-OH^-, their magnitude variation (within three times) is not as wide as those in the reactions of the carboxylic ester. Hence, the mere intermolecular nucleophilic attack mechanism (Figure 29 (a)) on the phosphate cannot account for this observation. In the BNP^- hydrolysis, the HO^--Zn^{II}-[12]aneN$_3$ species reacts faster than OH^- and HO^--Zn^{II}-[12]aneN$_4$. This is explained by the easiest formation of a transient five-coordinate, trigonal-bipyramidal phosphorus structure on Zn^{II}-[12]aneN$_3$ (Figure 29 (c)). The phosphate anion would be better accommodated on the more open coordination site of Zn^{II}-[12]aneN$_3$ than that of Zn^{II}-[12]aneN$_4$.

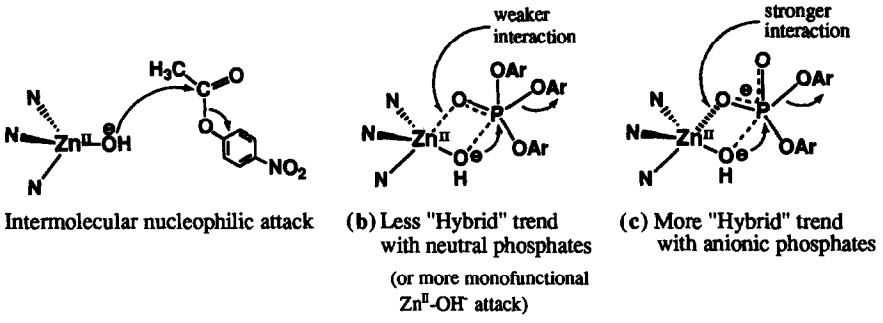

Figure 29. Three types of Zn^{II}-OH^- nucleophilic attack at esters

By contrast, in the TNP^0 hydrolysis the reaction rate order is OH^- > HO^--Zn^{II}-[12]aneN$_4$ > HO^--Zn^{II}-[12]aneN$_3$, the same as that for the carboxylic ester hydrolysis. However, the magnitude (within 3 times) for TNP^0 hydrolysis is not as wide as that for the carboxylic ester hydrolysis. So this reaction would take an intermediate path (Figure 29 (b)), where a less hybrid type of mechanism is operative, due to lesser interaction of neutral TNP^0 with the Zn^{II}.

The intermolecular nucleophilicity of these Zn^{II}-OH^- species may be compared with well studied $(NH_3)_5Co^{III}$-OH^-,[63] where neither has an extra vacant site for the prior carboxyester coordinations. As a nucleophile the HO^--Zn^{II}-[12]aneN$_3$ is ~ 1 order of magnitude more reactive than $(NH_3)_5Co^{III}$-OH^- toward the 4-nitrophenyl acetate substrate. The same direct nucleophilic mechanism was proposed for the Co^{III}-OH^-. Taking into consideration the charge and ligand field difference of the metal ions, this order of nucleophilicity seems reasonable.

Note the p*K*a of 6.4 for the Co^{III}-OH^- *vs.* 7.3 for the Zn^{II}-OH^-. Compared with free OH^- ion, the Zn^{II}-bound OH^- ion is ~ 250 times less reactive in 4-nitrophenylacetate hydrolysis. However, if the p*K*a values of 15.5 and 7.3 for free OH_2 and Zn^{II}-OH_2, respectively, are considered, *it is concluded that the Zn^{II}-OH^- would make a more effective nucleophile at neutral pH*. Probably, this is the most essential function of Zn^{II} in CA.

In the two typical carbonic anhydrase (CA)-catalyzing reactions (acetaldehyde hydration and carboxylic ester hydrolysis), the second-order kinetics and the plots of the rate constant *vs.* pH point to the same reaction mechanism as our model, involving the direct nucleophilic attack of Zn^{II}-OH^- at the carbonyl carbons, although our model rates are ca 10^4 times slower than those with CA.[44] Further structural modification of the basic structure of [12]aneN_3 by attachment of intramolecular bases to aid proton transfer (which is the rate-limiting in CA catalysis) or of other substituents for substrate recognition etc. is likely to create even better CA and other Zn^{II}-containing hydrolytic enzyme models.

4. New Biomimetic Synthesis of Cyclic Polyamines: Analogues of Spermine and Spermidine Alkaloids

Attachment of functional groups to macrocyclic polyamine skeletons had been almost unknown, except for the N-alkylation method.[64] A few years ago, we have discovered a new and versatile synthetic method that leads to a new class of macromonocyclic polyamines with side arms at a ring carbon. The reaction uses α,β-unsaturated carboxylic acid esters **62** and a linear polyamines **63** for a new one-step annulation that successively involves Michael addition, followed by intramolecular lactam formation (Figure 30).[65] The products from cinnamates **64** are reminiscent of cyclic spermine or spermidine alkaloids (*e.g.* **65**, **66**, **67**).[66,67] These alkaloids have some biological activities. Hence extension of these new synthetic macrocyclic polyamines may lead to appropriate drug candidates.

By this annulation method, various donor-pendant macrocycles were synthesized (**70** ~.**73**).[15,59,68-70] Moreover, starting from coumarin, we could directly synthesize phenol-pendant monooxocyclam **68** and then cyclam **69**.[71]

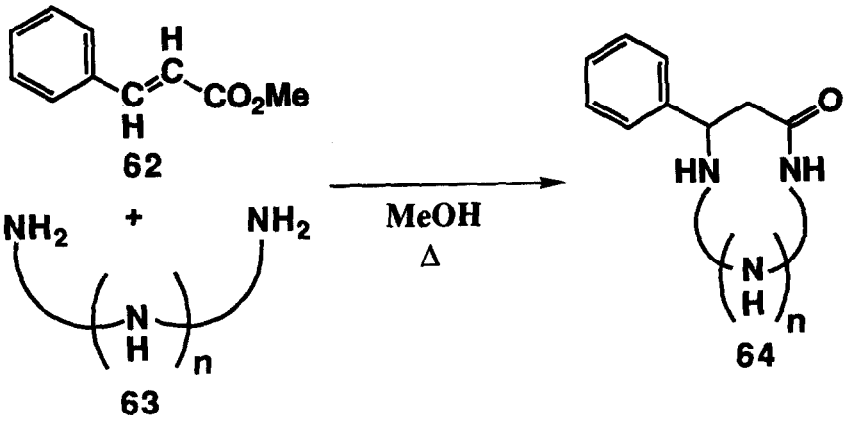

Figure 30. A new polyamine annulation method

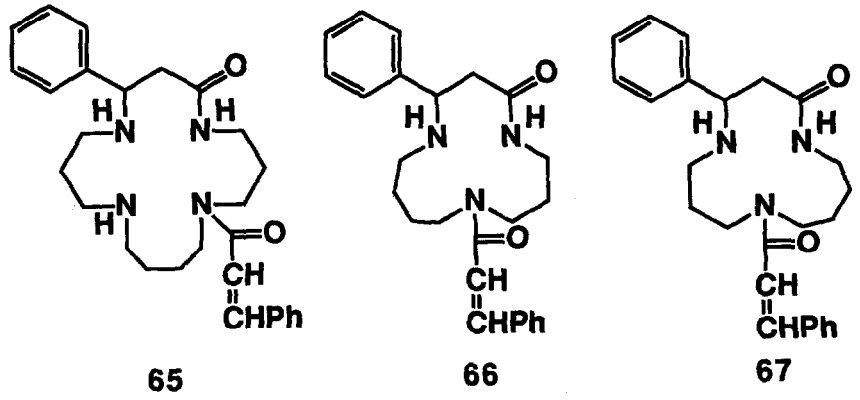

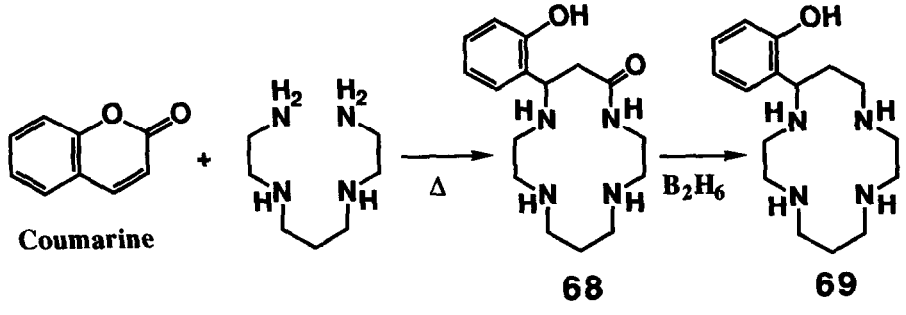

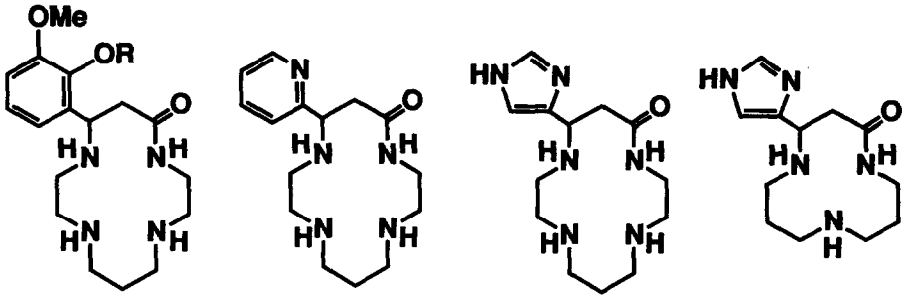

Not only biologically interesting, but also they are useful as precursors of donor pendant-attached cyclams. Thus, we could explore more functional macrocyclic polyamines with those new ligands. They are especially useful in building biomimetic metal complexes, **74**,[15] **75**,[68] **76**,[70] **77**[71] etc.. Interested readers are suggested to review these references.

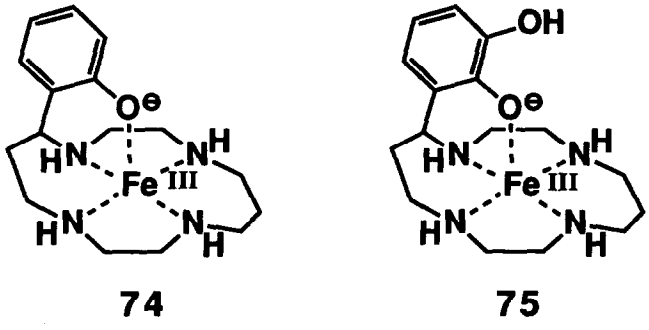

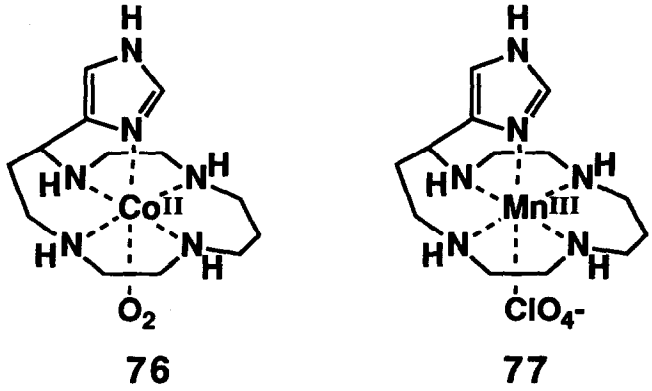

References

1. Stetter, H.; Mayer, K. M. *Chem. Ber.* **1961**, *94*, 1410.
2. Bosnich, B.; Poon, C. K.; Tobe, M. L. *Inorg. Chem.* **1965**, *2*, 1102.
3. For review: Curtis, N. F. *Coord. Chem. Rev.* **1968**, *3*,3.
4. (a) Pedersen, C. J. *J. Am. Chem. Soc.* **1967**, *89*, 2495.
   (b) Pedersen, C. J. *J. Am. Chem.* Soc. **1967**, *89*, 7017.
5. For review: Busch, D. H.; Farmecy, K.; Goedken, V.; Katovic, V.; Melnyk, A. C.; Sperati, C. R.; Tokel, N. In *Bioinorganic Chemistry,* Advances in Chem. Ser. **1971**, *100*, 44.
6. Collman, J. P.; Schneider, P. W. *Inorg. Chem.* **1966**, *5*, 1380.
7. Kodama, M.; Kimura, E. *J. Chem. Soc., Dalton Trans.* **1979**, 325.
8. Kodama, M.; Kimura, E. *J. Chem. Soc., Dalton Trans.* **1981**, 694.
9. Kimura, E.; Kodama, M.; Yatsumani, T. *J. Am. Chem. Soc.* **1982**, *104*, 3182.
10. Kimura, E. In *Biomimetic and Bioinorganic Chemistry*. Topics in Current Chemistry Vol 128, Springer Verlag, Heidelberg. **1985**, 113.
11. Zompa, L. J. *Inorg. Chem.* **1978**, *17*, 2531.
12. Bell, T. W.; Choi, H. -J.; Harte, W. *J. Am. Chem. Soc.* **1986**, *108*, 7427.
13. Smith, R. M.; Martell, A. E. In *Critical Stability Constants*; Plenum: New York, Vol. 5.
14. (a)Kodama, M.; Kimura, E. *J. Chem. Soc., Chem. Commun.* **1975**, 326.
    (b) Kodama, M.; Kimura, E. *J. Chem. Soc., Dalton Trans.* **1976**, 116.
15. Kimura, E.; Koike, T.; Uenishi, K.; Hediger, M.; Kuramoto, M.; Joko, S.; Arai, Y.; Kodama, M.; Iitaka, Y. *Inorg. Chem.* **1987**, *26*, 2975.
16. Kodama, M.; Kimura, E. *J. Chem. Soc.,Chem Commun.* **1975**, 891.
17. Kodama, M.; Kimura, E. *J. Chem. Soc.,Dalton Trans.* **1976**, 2341.
18. Delgado, R.; Fransto de Silva, J. J. R.; Vaz, M. C. T. A. *Inorg. Chim. Acta.* **1984**, *90*, 185.
19. Lan, S. J.; Kruck, T. P. A.; Sarkar, B. *J. Biol. Chem.* **1974**, *249*, 5878.
20. Pickart, L.; Freeman, J. H.; Loker, W. J.; Peisach, J.; Perkins, C. M.; Stenkamp, R. E.; Weistein, B. *Nature* **1980**, *288*, 715.
21. Kimura, E. *J. Coord. Chem., Sect B* **1986**, *15*, 1.

22. Machida, R.; Kimura, E.; Kodama, M. *Inorg. Chem.* **1983**, *22*, 2055.
23. Kimura, E.; Lin, Y.; Machida, R.; Zenda, H. *J. Chem. Soc., Chem. Commun.* **1986**, 1020.
24. Kimura, E.; Dalimunte, C. A.; Yamashita, A.; Machida, R. *J. Chem. Soc., Chem Commun.* **1985**, 1041.
25. Kimura, E.; Kurogi, Y.; Wada, S.; Shionoya, M. *J. Chem. Soc., Chem. Commun.* **1989**, 781.
26. Kimura, E.; Kurogi, Y.; Tojo, T.; Shionoya, M.; Shiro, M. *J. Am. Chem. Soc.* **1991**, *113*, 4857.
27. Margerum, D. W.; Dukes, G. R. In *Metal Ions in Biological Systems*, Sigel, H. Ed., Marcel Dekker, New York 1974, Vol 1, 157.
28. Murray, S. G.; Hartley, F. R. *Chem. Rev.* **1981**, *81*, 365.
29. Kimura, E.; Kurogi, Y.; Takahashi, T. *Inorg. Chem.* **1991**, *30*, 4117.
30. Kimura, E.; Kurogi, Y. unpublished results.
31. Kimura, E.; Kimura, Y.; Yatsunami, T.; Shionoya, M.; Koike, T. *J. Am. Chem. Soc.* **1987**, *109*, 6212.
32. Izatt, R. M.; Bradshaw, J. S.; Nielsen, S. A.; Lamb, J. D.; Christensen, J. J. *Chem. Rev.* **1985**, *85*, 271.
33. Kimura, E.; Sakonaka, S.; Machida, R.; Kodama, M. *J. Am. Chem. Soc.* **1982**, *104*, 4255.
34. Kushi, Y.; Machida, R.; Kimura, E. *J. Chem. Soc., Chem. Commun.* **1985**, 216.
35. Machida, R.; Kimura, E.; Kushi, Y. *Inorg. Chem.* **1986**, *25*, 3461.
36. Kimura, E.; Machida, R.; Kodama, M. *J. Am. Chem. Soc.* **1984**, *106*, 5497.
37. Kimura, E.; Machida, R. *J. Chem. Soc., Chem. Commun.* **1984**, 499.
38. Bertini, I.; Luchinat, C.; Maret, W.; Zeppezarer, M. (Eds) In *Zinc Enzymes*; Birkhänser, Boston, MA, **1986**.
39. Vallee, B. L.; Galdes, A. *Adv. Enzymol.* **1984**, *56*, 283.
40. Bertini, I.; Luchinat, C. *"The Enzymatic Catalyst of Hydrolytic and Other Reactions"* to be published. This author expresses thanks to Prof. Bertini for giving permission to review his manuscript before publication.

41. Clewley, R. G.; Slebocha-Tilk, H.; Brown, R. S. *Inorg. Chim. Acta.* **1987**, *157*, 233

42. Read, R. J.; James, M. N. G. *J. Am. Chem. Soc.* **1981**, *103*, 6947.

43. Woolley, P. *Nature (London)* **1975**, *258*, 677.

44. Kimura, E.; Shiota, T.; Koike, T.; Shiro, M.; Kodama, M. *J. Am. Chem. Soc.* **1990**, *112*, 5805.

45. (a) Norman, P. R. *Inorg. Chim. Acta.* **1987**, *130*, 1.
(b) Norman, P. R.; Tate, A.; Rich, P. *Inorg. Chim. Acta.* **1988**, *145*, 211.

46. Gellman, S. H.; Petter, R.; Breslow, R. *J. Am. Chem. Soc.* **1986**, *108*, 2388.

47. Breslow, R.; Berger, D.; Huang, D-L. *J. Am. Chem. Soc.* **1990**, *112*, 3686.

48. Pocker, Y.; Stone, J. T. *Biochemstry* **1968**, *7*, 2936.

49. Kimura, E.; Koike, T. *Comments Inorg. Chem.* **1991**, *11*, 285.

50. Schaber, P. M.; Fettienger, J. C.; Churchill, M. R.; Nalewajek, D.; Fries, K. *Inorg. Chem* **1988**, *27*, 1641.

51. Kimura, E.; Koike, T.; Shionoya, M.; Shiro, M. *Chem. Lett.*, in press.

52. Eriksson, A. E.; Kylsten, P. M.; Jones, T. A.; Liljas, A. *Proteins.* **1988**, *4*, 283.

53. Koike, T.; Kimura, E.; Nakamura, I.; Hashimoto, Y.; Shiro, M. paper submitted.

54. (a) Ferrer, S.; Borras, J.; Miratvilles, C.; Fuertes, A. *Inorg. Chem.* **1989**, *28*, 160.
(b) Ferrer, S.; Borras, J.; Miratvilles, C.; Fuertes, A. *Inorg. Chem.* **1990**, *29*, 206.

55. Pocker, Y.; Stone, J. T. *Biochemistry* **1967**, *6*, 668.

56. Taylor, P. W.; King, R. W.; Burgen, A. S. V. *Biochemistry,* **1970**, *9*, 2638.

57. Kimura, E.; Yamaoka, M.; Morioka, M.; Koike, T. *Inorg. Chem.*, **1986**, *25*, 3883.

58. Kimura, E.; Koike, T.; Toriumi, K. *Inorg. Chem.*, **1988**, *27*, 3687.

59. Kimura, E.; Kurogi, Y.; Shionoya, M.; Shiro, M. *Inorg. Chem.*, **1991**, *30*, 4524,

60. Kimura, E.; Koike, T.; Shiota, T.; Iitaka, Y. *Inorg. Chem.*, **1990**, *29*, 4621.

61. Rogers, J. I.; Mukherjee, J.; Khalifah, R. G. *Biochemistry* **1987**, *26*, 5672.

62. Koike, T.; Kimura, E. *J. Am. Chem. Soc.* **1991**, *113*, 8935.

63. Sargeson, A. M.; Harrowfield, J. M.; Norris, V. *J. Am. Chem. Soc.* **1976**, *98*, 7282.

64. (a) Wagner, F.; Mocella, M. T.; D'Aniello, M. J.,Jr.; Wang, A. H.-J.; Barefield, E. E. *J. Am. Chem. Soc.* **1974**, *96*, 2625.
(b) Wagner, F.; Barefield, E. E. *Inorg. Chem.* **1976**, *15*, 408.

(c) Barefield, E. K.; Freeman G. M.; Van Derveer, D. G. *Inorg. Chem.* **1986**, *25*, 552.

65. (a) Kimura, E. *Pure and Applied Chem.* **1986**, *58*, 1461.

    (b) Kimura, E. *ibid*, **1989**, *61*, 823.

66. Seifert, K.; Johne, S.; Hesse, M. *Helv. Chim. Acta.* **1982**, *65*, 2450.

67. Smith, T. A. In *Progress in Phytochemistry*, Vol. 4, Pergamon Press, **1977**, p 27.

68. Kimura, E.; Joko, S.; Koike, T.; Kodama, M. *J. Am. Chem. Soc.* **1987**, *109*, 5528.

69. Kimura, E.; Koike, T.; Nada, H. *J. Chem. Soc., Chem. Commun.* **1986**, 1322.

70. Kimura, E.; Shionoya, M.; Mita, T.; Iitaka, Y. *J. Chem. Soc., Chem. Commun.* **1987**, 1712.

71. Kimura, E.; Koike, T.; Takahashi, M. *J. Chem. Soc.,Chem Commun.* **1985**, 385.

72. Kimura, E.; Shionoya, M.; Yamauchi, T.; Shiro, M. *Chem. Lett.*, **1991**, 1217.